DEVELOPMENT OF TRANSMITTER FOR SEABED LOGGING (SBL) IN REAL AND SCALED ENVIRONMENT

By

NUR ADILAH BINTI ZAINON

Dissertation Report Submitted in Partial Fulfillment of
the Requirements for the
Bachelor of Engineering (Hons)
(Electrical & Electronics Engineering)

MAY 2011

Universiti Teknologi PETRONAS
Bandar Seri Iskandar
31750 Tronoh
Perak Darul Ridzuan

CERTIFICATION OF APPROVAL

DEVELOPMENT OF TRANSMITTER FOR SEABED LOGGING (SBL) IN REAL AND SCALED ENVIRONMENT

By

NUR ADILAH BINTI ZAINON

Dissertation Report Submitted in Partial Fulfillment of
the Requirements for the
Bachelor of Engineering (Hons)
(Electrical & Electronics Engineering)

Approved by,

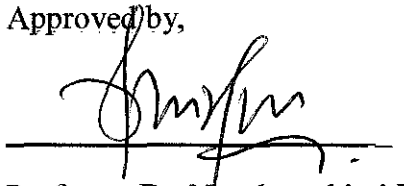

Professor Dr. Noorhana binti Yahya
Professor Dr. Noorhana Yahya
Project Supervisor
Faculty of Science & Information Technology
Universiti Teknologi PETRONAS

UNIVERSITI TEKNOLOGI PETRONAS
TRONOH, PERAK

MAY 2011

CERTIFICATION OF ORIGINALITY

This is to certify that I am responsible for the work submitted in this project, that the original work is my own except as specified in the references and acknowledgements, and that the original work contained herein have not been undertaken or done by unspecified sources or persons.

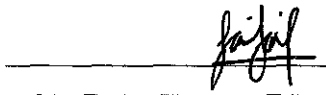

NUR ADILAH BINTI ZAINON

ABSTRACT

Electromagnetic (EM) technology called Seabed Logging (SBL) has recently been used for hydrocarbon exploration. Seabed logging (SBL) is an application of marine controlled source electromagnetic (CSEM) method which is used to detect the location of oil reservoir. A recently developed transmitter is using Horizontal Electric Dipole (HED) transmitter based on electromagnetic (EM) surveying technique. The technique has proven particularly useful for detecting thin and highly resistive layers of hydrocarbon reservoirs. However, to detect the hydrocarbon reservoirs at very deep seawater still remains a challenge. There are many limitations of the conventional HED transmitter in terms of depth penetration for deep target (~2.5km). This project has come out to further improve the current design of transmitter that can penetrate more below the seafloor. This project consists of simulation and modeling the prototype of EM antenna. Aluminum is the best material to this design since it is easy to fabricate, light, cheaper than copper and has high resistive corrosion. The shape of half ring antenna gives greatest improvement on the amplification of 102.19% as compared to the straight shape and 20.66% compared to ring shape. Further improvement to the current design was done by combining four half ring antennas which is called Quadrapole antenna. The Quadrapole antenna with parallel connection and feeding points at the center gives percentage difference of 196.77.88%. The combination of magnetic feeders and Quadrapole antenna enhance the output of EM wave with 445.76% increment compared to the Quadrapole antenna without magnetic feeders.

ACKNOWLEDGEMENT

I would like to express my gratitude to all those who help me to complete this Final Year Project II (FYP II). First of all, I want to express my deepest appreaciation to my supervisor, Professor Dr. Noorhana Yahya for her dedication, motivation, guidance and crucial contribution towards this project. Furthermore, I would like to thank the postgraduate students and my colleagues for their support, assistance and encouragement. Last but not least, I would like to give my special thanks to all my family members especially my beloved mother and father, also my brother and sister for their motivation and emotion support.

Thank you.

TABLE OF CONTENTS

LIST OF FIGURES

LIST OF TABLES

LIST OF ABBREVIATIONS

SBL	Seabed Logging
EM	Electromagnetic
HED	Horizontal Electric Dipole
Hz	Hertz
CSEM	Marine Controlled Source Electromagnetic
CST	Computer Simulation Technology
DAS	Decaport Data Acquisition System

CHAPTER 1

INTRODUCTION

1.1 Background of Study

Nowadays, every machine requires energy to operate and many of these machines runs on fuel. Fuel is a form of energy extracted from crude oil. Crude oil or in other word petroleum can be found onshore and offshore [1]. Petroleum consists mainly from hydrocarbon. A hydrocarbon is an organic compound consisting entirely of hydrogen and carbon. The hydrocarbon has a high resistive value which current are unable to flow. Some research has been done regarding the resistivity of the hydrocarbon. In petroleum exploration, reservoirs are detected based on the different resistivity of the sea level [2]. However, the exploration of hydrocarbon is a difficult task for oil and gas company. Long time ago, seismic technology has been widely used to search for workable drilling wells. However, well drilling is relatively expensive and by depending on the seismic data, the success rate is only about 10-30% accuracy [3].

Detecting and assessing hydrocarbon reservoirs without the need to drill test wells is of major importance to the petroleum industry [4]. During the past several years, we have seen an increasing focus on the use of CSEM technology for hydrocarbon exploration in marine environments and, recently, a number of success stories have been published. The technology has been demonstrated to aid both detection and delineation of hydrocarbon-filled reservoirs [5].

Seabed Logging (SBL) is an application of the marine controlled source electromagnetic (CSEM) method that is used to directly detect and characterize possible hydrocarbon-bearing prospects. Although the CSEM method has been used by academia

for more than three decades, the application as a direct hydrocarbon indicator was first introduced about five years ago. Since SBL introduced, locations of hydrocarbon reservoir had been discovered is very promising. It first had been introduce in 2002, and now the application is growing increasingly. The central idea of SBL is the guiding of electromagnetic energy in thin resistive layers within conductive sediments [6]. This EM technique for marine hydrocarbon prospecting, first used commercially in November 2002, identifies resistive reservoirs by measuring the energy received at long source-receiver offset distance [7] The implication is that the EM data have the potential to increase the detection rates by 50% or even more [8]. The basis of the approach is the use of a mobile horizontal electric dipole (HED) source and an array of seafloor electric field receivers [9].

Referring to Figure 1, the transmitting dipole emits a low frequency electromagnetic signal that diffuses outwards both into the overlying water column and downwards into the seabed. Electromagnetic (EM) energy is rapidly attenuated in the conductive seafloor sediments, but in a thin and high resistive layer (e.g. a hydrocarbon reservoir ~20-1000Ωm), EM energy is attenuated less and propagation is more efficient along the layer. The signal will be guided horizontally along a reservoir and reflected back to the seafloor [10]. It makes contrast for about 400 scaled as compared to the resistivity of the seawater which is only 0.25Ωm. [11]

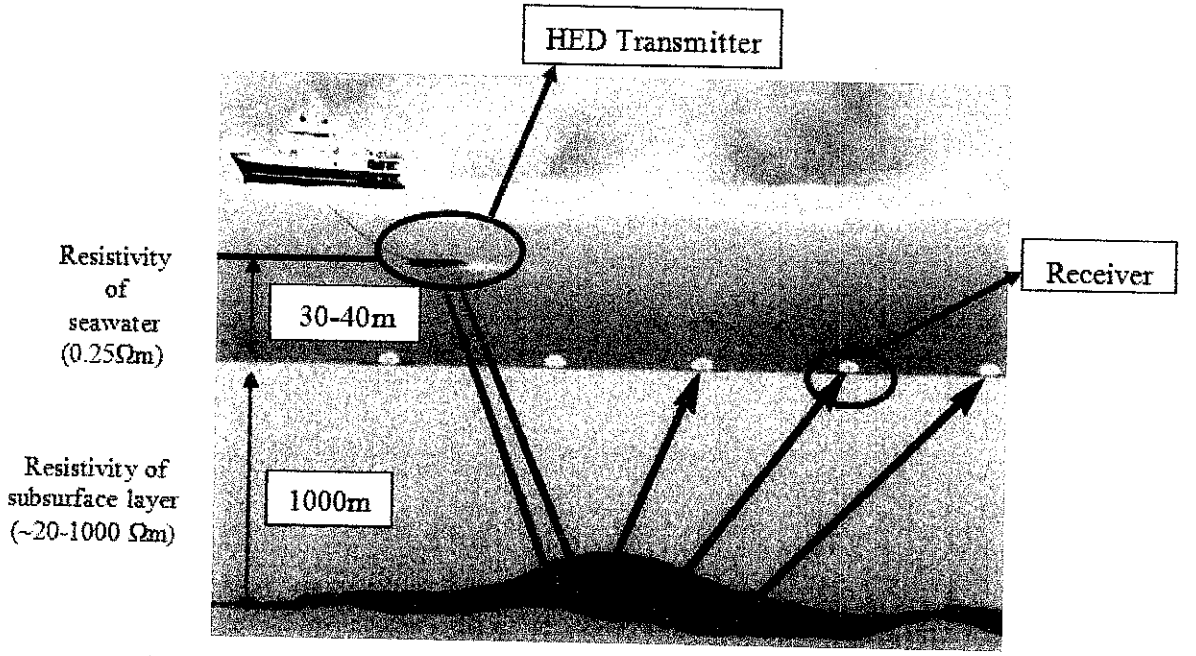

Figure 1: Location of HED transmitter and receiver based on SBL method [12]

Guided EM energy is constantly refracted back to the seafloor and the signal is then be recorded by stationary seafloor receivers having both magnetic and electric dipole antennas [13]. The recorded data will be sent to the surface for further data analysis. This is how the current technology is used to detect hydrocarbon reservoir [14].The use of sea bed logging is currently revolutionizing the exploration for hydrocarbons. It remains to be seen if this new method will revolutionize the production of oil and gas [15].

1.2 Problem Statement

1.2.1. Problem Identification

In seabed logging, the technology used is applied for deep seawater oil exploration. But there are many limitations of the conventional HED transmitter in terms of depth penetration for deep target (~2.5km). Many researchers are now investigating new method in overcoming those problems. However this project could provide a solution to the limitations suffered in seabed logging.

1. The basis of the approach is the use of Horizontal Electrical Dipole (HED) which emits a low frequency electromagnetic (EM) signal into the underlying seabed and downwards. However, some of the signal also goes upward because the signal can come from any direction since this types of antenna less focused and radiates equally in all directions.

1.3 Objective and Scope of Study

Since the current technology has its own disadvantages, therefore a new method must be developed to overcome those problems and consequently increase the production in oil exploration process. There are three main objectives for this project. Below also described all the main objectives.

1. To design more 'focused' transmitter

In seabed logging, EM wave is the main factor in the whole process. One of the aims of antenna engineering is to design antennas which transmit most of their radiation in a particular direction. With directivity of antenna, we can concentrate the EM wave downwards into the seabed and may enhance the EM propagation wave.

2. To develop scaled factor

The antenna needs to be up-scaled as comparable to the size of the scaled model so that it could drive more input current signal. Here the scaled model has to be enlarged and so that the scaled factor is decrease. Studies must also be conducted to change the frequency which has to be reduced with the increasing size of the scaled model. Without changing the current situation, a very high saturation of electromagnetic wave will be circulating along the antenna and limits them to go further.

3. To measure magnetic field

Magnetic field produced from EM wave can be sensed by fluxgate magnetic field sensor. This sensor is then connected to the decaport data acquisition system (DAS) Model NI PXI-1042 for the configuration purposes.

The area of study for this project will be divided into two parts. First part is doing simulation of antenna design and second part is modeling the prototype of EM antenna. Before fabrication of the antenna take place, simulation to design the antenna will be done first. A new design of EM transmitter will be developed by using CST software. Afterwards the experimental work will be performed to validate the data simulation by producing prototype and testing the capability of transmission of EM wave.

CHAPTER 2

LITERATURE REVIEW

2.1 Seismic Technology

The first oil field found by seismic exploration alone was the Seminole field of Oklahoma in 1928 [16]. Understanding of seismic method is an important aspect to know its disadvantages compared with the sea bed logging method. The acoustic characteristic of seismic wave plays a major role to determine hydrocarbon formation. Basic idea to describe seismic propagation to the rock or sediment is low frequency sound waves are generated at the surface by a high energy source. They travel down through the earth, and are reflected back from the tops and bases of layers of rock where there is a change in rock properties. The reflected sound travels back to the surface and is recorded by receivers resembling microphones. The time taken for the sound to travel from the source down to the reflecting interface and back to the surface tells us about the change of rock properties across the interface. After a received seismic signal had been analyse, the interpreted data is valuable for determine the hydrocarbon reservoir. Two types of direct hydrocarbon indicates on a seismic record are bright spots and flat spots. A flat spots is a level, flat seismic reflector in a petroleum trap formed by rock layers that are not flat such as anticline. The flat spot is a reflection of a gas-oil. Even bright spot have been used very successfully to locate gas reservoirs and gas caps on saturated oil fields. Not all bright spots however are commercial deposits of natural gas. A dim spot where the reflection amplitude becomes less occurs over same reefs. This is where the defect of the seismic method can lead to the misinterpretation and increase the risk of drilling exploration well. Value of seismic data is sometimes limited in when it comes to discriminating between residual hydrocarbons, such as where the reservoir seal has been breached, and commercial saturations of hydrocarbons. This is where SBL data needs to

attached with the data from seismic to gain accurate prospect of hydrocarbon filled layers by information from the data anomaly [17].

2.2 Seabed logging

Seabed Logging was introduced to oil industry just two years ago. The new technology would make it possible to identify the presence of oil and gas in undrilled prospects. In seabed logging electromagnetic waves are used to monitor possible hydrocarbons in reservoir beneath the sea floor. In much the same way as radio signals are transmitted, electromagnetic waves are sent out from a vessel. The transmitter is dragged along after the boat, about 30 meters above the sea floor. If the signals meet water in the reservoir the signals are not reflected. However, if they reach hydrocarbons the radio waves send signals back to the receivers on the floor bed. Based upon the fact, all geological media have some sort of electrical conductivity [15]. The conductivity of geological medias such as limestone, sandstone and slate, which are the most common ones beneath the seabed floor, varies little. But if the sandstone is filled with oil, the conductivity is radically reduced. The radio waves are then reflected back. If the sandstone is filled with water, however, the conductivity is high, and the waves are therefore not reflected [18].

The basis of the approach is the use of Horizontal Electrical Dipole (HED), which is towed a little above (~30m) the seafloor by an acquisition vessel. The towed emits a low frequency electromagnetic (EM) signal that couples with the surrounding water and then into the underlying seabed and downwards. Some of the signal also goes upward. Referring to Figure 2, this "air signal" starts to interfere with the geological signal as the water depth decreases and, if present, must be removed during processing. It is an area of ongoing research and currently limits the SBL technique to a minimum of about 200m water depth. The air wave component depends on water depth, source-receiver range, frequency and seabed resistivity.

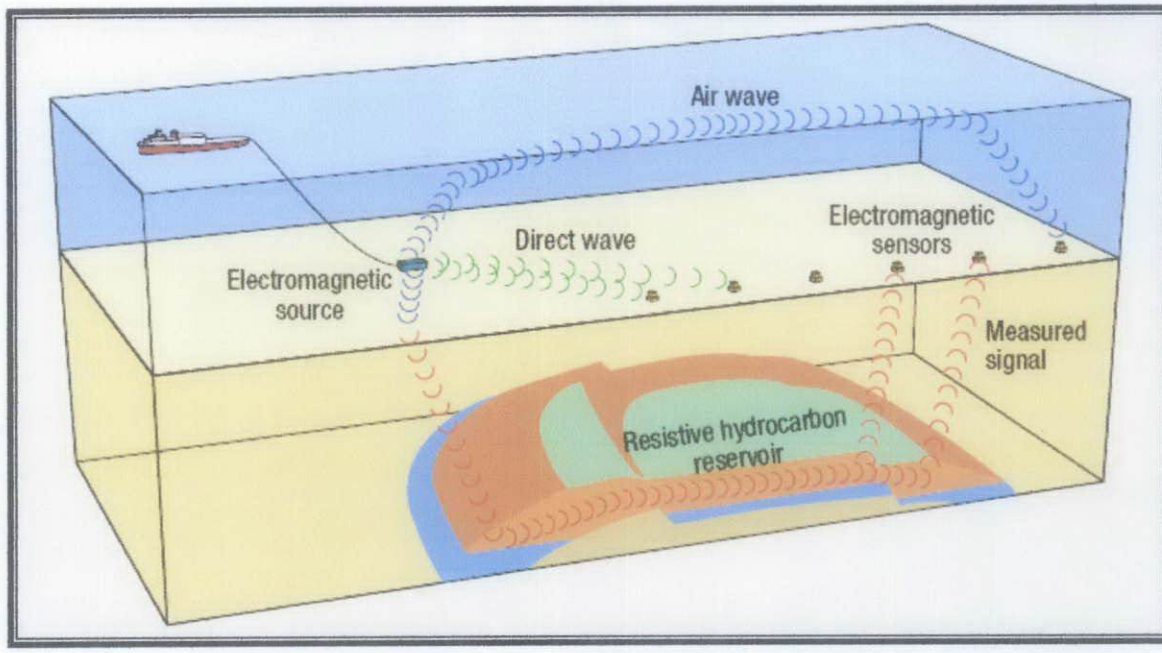

Figure 2: The direction of air wave, direct wave and measured wave

In practice, a low frequency EM signal must be generated, typically between 0.25-10Hz, to allow penetration to 2500-3000m into the subsurface. At low frequencies, the EM field diffuses, leading to strong dispersion. Energy is constantly returned back to the seafloor and is detected by dipole receivers placed on the seafloor. Both the amplitude and the phase of the received signal depend on the resistivity structure beneath the seabed. The sail line starts at about 10km before the first receiver and ends about 10km after the last receivers. This ensures that all receivers have active source data with source-receiver offsets of 10km. When the source-receiver distance is larger than the reservoir depth, energy from the resistive layer will dominate the directly transmitted energy [19].

Sea Bed Logging can be divides in two types of EM wave source which are man-made EM source in term Controlled Source Electromagnetic Method (CSEM) and Magneto telluric Method (MT) that using the natural source of EM. The principal of transmitting and detecting of EM wave from both methods are same. The difference is only on how the EM wave is generated [20].

2.3 Controlled Source Electromagnetic (CSEM)

The marine Controlled Source Electromagnetic (CSEM) technique was developed almost three decades ago to study the conductivity structure beneath the seafloor. Recently the marine CSEM technique was applied commercially to the problem of detecting the presence of hydrocarbon filled layers in the sub-sea formations and a number of companies are now providing this service. The marine CSEM technique for remote and direct identification of hydrocarbon filled layers in deepwater areas uses a mobile horizontal electric dipole (HED) source, located slightly above the sea-floor, and an array of electric and magnetic dipole field receivers located directly on the seafloor [21].

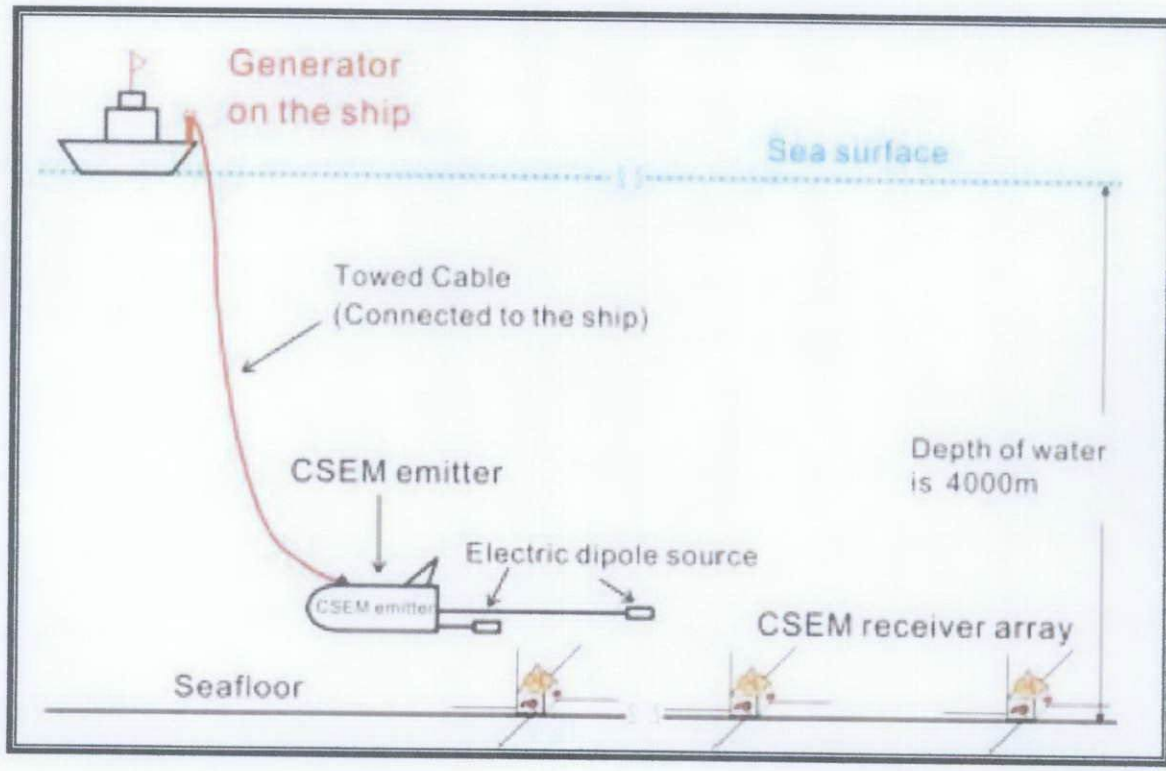

Figure 3: Working principle of marine CSEM system [22]

There are few explanations from field expertise regarding how is SBL operates. Andy Overton of Offshore Hydrocarbon Mapping (OHM) from interview, [23] CSEM is based on a low-frequency electromagnetic signal coming from a towed source which is transmitted through the seafloor to an array of multicomponent electromagnetic receivers placed on the seabed. Since the direct signal through the water is rapidly attenuated, the signals arriving at the receiver are dominated by fields that have interacted with the earth, so the bulk electrical resistivity of the subsurface can be determined. This resistivity is modified by the presence of subsurface resistive layers, and because hydrocarbons increase the resistivity of a formation by 1 to 2 orders of magnitude, these changes can be detected and logged by the receivers. A CSEM survey can therefore indicate the presence of oil and gas in an offshore reservoir, and also help outline the edges of an accumulation.

On the other hand, T.Eidesmo, S.Ellingsrud, L.M.MacGregor, S.Constable, M.C.Sinha, S.Johansen, F.N. Kong and H.Weterdahl [24] also explain the method on how EM penetrates the overburden and reflected back to the EM receiver. The basis of the approach is the use of a mobile horizontal electric dipole (HED) source and an array of seafloor electric field receivers. The transmitting dipole emits a low frequency (typically a few tenths to a few tens of Hz) electromagnetic signal that diffuses outwards both into the overlying water column and downwards into the seabed. The rate of decay in amplitude and the phase shift of the signal are controlled both by geometric and by skin depth effects. Because in general the seabed is more resistive than seawater, skin depths in the seabed are longer. As a result, electric fields measured at the seafloor by a receiving dipole at a suitable horizontal range are dominated by the components of the source fields that have followed diffusion paths through the seabed. In this explanation, there was a term skin depth effect was highlighted. Since it was deployed in the actual task, SBL method showed a promising result in finding hydrocarbon [25].

Table 1: Literature Review Summary

Controlled Source Electromagnetic (CSEM)	Seismic Technology
1. CSEM technique was developed to study the conductivity structure beneath the seafloor. 2. Nowadays, CSEM technique was applied in oil and gas industry to detect the presence of hydrocarbon filled layers beneath the seafloor.	1. Seismic used sound waves to determine hydrocarbon formation. 2. The time taken for the sound to travel from the source down to the reflecting interface and back to the surface tells the change of properties across the interface. 3. The analyzed data will determine the presence of hydrocarbon reservoir.

2.4 Electromagnetic (EM) Wave

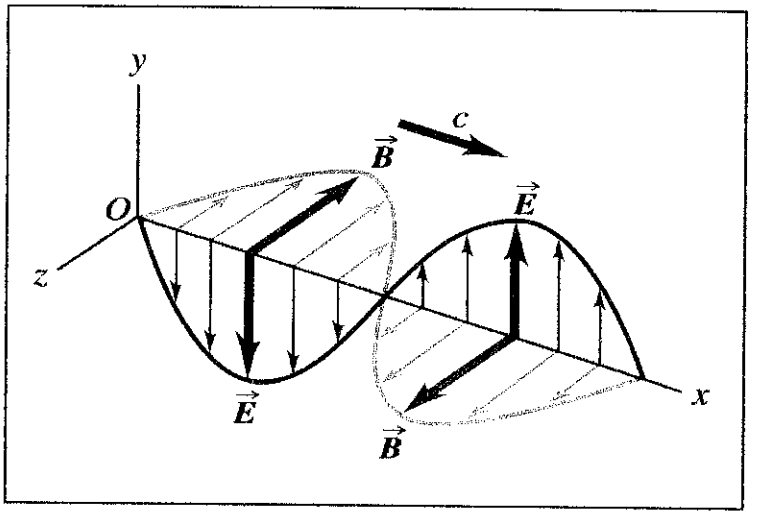

Figure 4: Propagation of electromagnetic wave

EM wave is a wave generated when current runs through a path. Upon that phenomenon, electric field and magnetic field is created perpendicular to each other [26]. The propagation of electromagnetic (EM) waves is governed by Maxwell's equations, which encapsulate the connection between the electric field and electric charge, the magnetic field and electric current, and the bilateral coupling between the electric and magnetic field quantities.

Referring to Figure 4, electrical field and magnetic field are perpendicular to each other. Maxwell's equations hold in any material, including free space, and at any spatial location in an arbitrary (x,y,z) coordinate system [27] .The general form of Maxwell's equations are written as

$$\nabla \cdot \vec{D} = \rho_v \tag{1}$$

$$\nabla \times \vec{E} = -\frac{\partial \vec{B}}{\partial t} \tag{2}$$

$$\nabla \cdot \vec{B} = 0 \tag{3}$$

$$\nabla \times \vec{H} = \vec{J} + \frac{\partial \vec{D}}{\partial t} \tag{4}$$

where

D = electric flux density

E = electric field intensity

and $D = \varepsilon E$, where ε = electrical permittivity of the medium

B = magnetic flux density

H = magnetic field intensity

and $B = \mu H$, where μ = magnetic permeability of the medium

J = current density per unit area

ρv = electric charge density per unit volume

These equations form the basis for electromagnetic waves and radiation and can be considered as a law to understand electrodynamics. Maxwell's equations are a system differential equations which show how electrical and magnetic fields are dependent on each other and on electrical charge and current [28].

2.5 Biot-Savart Law

The Biot-Savart Law is an equation in electromagnetism that describes the magnetic field, B generated by an electric current. When a linear conductor is carrying a current I, there is a magnetic flux density is induced around the conductor [28].The phenomenon is illustrated in figure below:

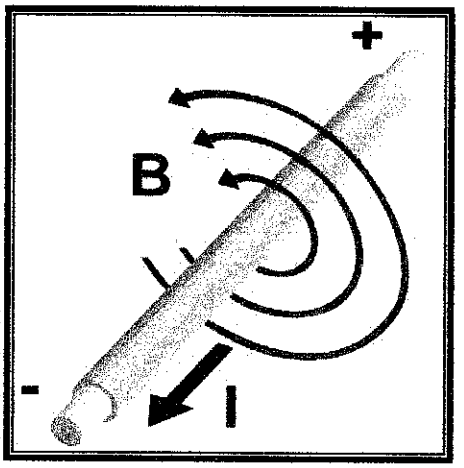

Figure 5: An electric current produces magnetic field [29]

From the Biot-Savart Law equation, we can determine the strength of the magnetic flux density B by this following equation:

$$\vec{B} = \mu_0 \vec{H} = \hat{\phi} \frac{\mu_0 I}{2\pi r} \tag{5}$$

Where r is the distance between antenna and the point in space, μ_o is permeability in free space [28]. Based on this equation, when the distance between antenna and the point of space increased, the magnetic flux density will decreased. The current supply is proportional to magnetic flux density, hence when the value of I is increased, B will also be increased.

2.6 Lenz's Law

Lenz's Law states that an induced electromotive force generates a circuit that induces a counter magnetic field that opposes the magnetic field generating the current. See figure below.

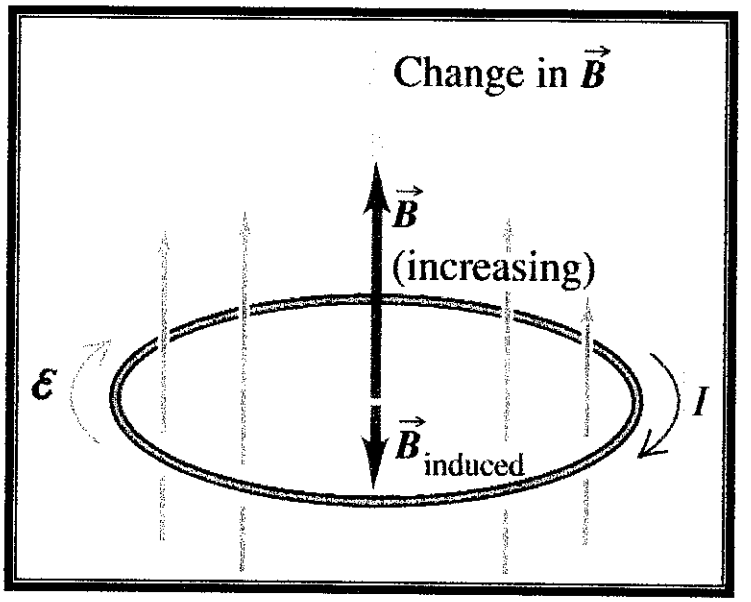

Figure 6: Lenz Law illustration

This means that the B field induces current, I in the clockwise direction. The current in turn induce a B field in the onward direction, which opposes the original field that was initially going up. It is this opposition that we are concerned about in our fluxgate sensor. When the external EM signal comes into contact with the induced B field, it will cause a disturbance which will make a difference in the voltage being measured [30].

2.7 Electrical Properties of Material

The conductivity of a material is a measure of how easily electrons can travel through the material under the influence of an external electric field [28]. In other words, conductivity is the ability of the material to conduct the current flow. It is very important to use antenna from higher conductivity material since the EM wave strength is depends on current flow. The table below shows conductivity of some common conductor at 20°C.

Table 2: Conductivity of some common materials at 20°C [28]

MATERIAL	CONDUCTIVITY, σ (S/m)
Silver	6.2×10^7
Copper	5.8×10^7
Gold	4.1×10^7
Aluminium	3.5×10^7
Iron	10^7
Mercury	10^7
Carbon	3×10^4

2.8 EM Transmitter

EM transmitter is defined as a radial waveguide that generates the EM wave [31]. Usually an EM transmitter uses turns of coil to generate the electromagnetic wave that is at a single frequency. When we apply a high frequency source of alternating voltage input to the coils/winding of the transmitter, a magnetizing current is developed in the winding itself. This magnetizing current then will generate an alternating flux in

the magnetizable core that links the winding in order to develop an alternating polarity output voltage [32].

The amount of current induced depends on the electrical conductivity of the material itself. Commonly we use copper as the transmitter since it is a highly electrically conductive material. The currents induced in the transmitter then will generate a secondary EM field that can be detected using a receiver [33].

2.9 Directivity on Antenna

There are various kinds of ways to manipulate a radiation pattern to meet the demands of a specific task [34]. Directivity is a fundamental antenna parameter. It is a measure of how 'directional' an antenna's radiation pattern is. An antenna that radiates equally in all directions would have effectively zero directionality, and the directivity of this type of antenna would be 1 (or 0 dB) [35]. Figure below shown 2 radiation patterns:

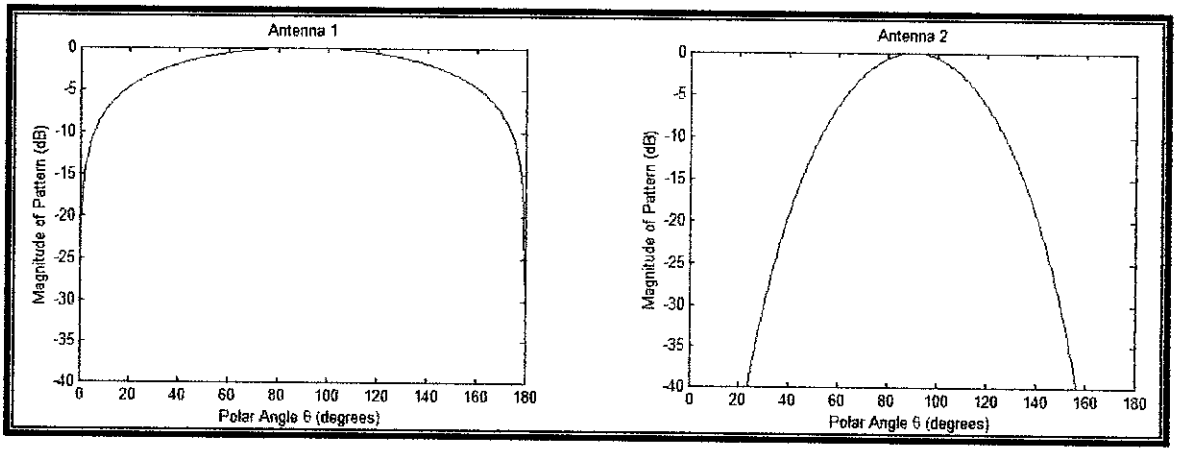

Figure 7: Radiation Patterns [35]

By comparing both of these patterns, antenna 2 implies a more 'focused' antenna. Therefore can produce higher magnitude and capable enough to transmit most of their radiation in a particular direction.

2.10 Skin Depth

This theory states the capability of electromagnetic wave penetrate a medium [36]. The skin depth is the measure of the distance over which the current falls to 1/e of its original value. In other words, "skin depth" can be expressed by the limit to how far EM wave can be transmitted. The skin depth is a property of the material that varies with the frequency of the applied wave. In propagating the EM wave, there is attenuation that needs to take into consideration. The attenuation of EM wave is the main factor that determines the distance of the EM wave transmission. The attenuation differs from the medium of propagation and also the frequency applied by the transmitter [37]. As EM wave penetrate into medium, the wavelength is shortened and the amplitude rapidly attenuated. Skin depth and wavelength will depend on frequency and medium parameters, σ = conductivity [38]. Skin depth and wavelength is given by:

Skin Depth:

$$\delta = \sqrt{\frac{2}{\mu\sigma\omega}} \tag{6}$$

Wavelength:

$$\lambda = 2\pi\sqrt{\frac{2}{\mu\sigma\omega}} \tag{7}$$

Where:

δ = skin or penetration depth

$\omega = 2\pi f$, f = frequency

σ= conductivity [Siemens/meter, S/m]

$\mu = \mu_o$ = permeability of vacuum = $4\pi 10^{-7}$ [Henry/meter]

Hence, in order to increase the skin depth, the wavelength should be higher and the frequency used to transmit the EM wave should be lower [39].

2.11 Scaled Model Calculation

A scale model is a physical model, a representation or copy of an object that is larger or smaller than the actual size of the object, which seeks to maintain the relative proportions (the scale factor) of the physical size of the original object. Very often the scale model is smaller than the original and used as a guide to making the object in full size. Scale models are built or collected for a reason. We require scale models to test the likely performance of a particular design at an early stage of development without incurring the full expense of a full-sized prototype [40].

Based on the skin depth formula, the ratio of the full scale and the laboratory scale dimensions is

$$\frac{\delta_{fs}}{\delta_{lab}} = n$$

$$\text{Skin Depth} \quad \delta = \sqrt{\frac{2}{\mu\sigma\omega}}$$

$$\frac{\left[\sqrt{\frac{2}{\mu\sigma\omega}}\right]_{fs}}{\left[\sqrt{\frac{2}{\mu\sigma\omega}}\right]_{lab}} = n$$

since $\boxed{\frac{1}{\rho} = \sigma}$ $\boxed{\omega = 2\pi f}$

$$\frac{\left[\sqrt{\frac{2\rho}{\mu 2\pi f}}\right]_{fs}}{\left[\sqrt{\frac{2\rho}{\mu 2\pi f}}\right]_{lab}} = n$$

$$\left[\frac{2\rho}{\mu 2\pi f}\right]_{fs} = n^2 \left[\frac{2\rho}{\mu 2\pi f}\right]_{lab}$$

The full scale and the laboratory scale both generally concerned with nonmagnetic conductors $\mu=\mu_0$ the permeability of the free space, so that

$$\left(\frac{\rho}{f}\right)_{fs} = n^2 \left(\frac{\rho}{f}\right)_{lab}$$

Assume value of ρ is same,

So for the frequency

$$\left(\frac{1}{f}\right)_{fs} = n^2 \left(\frac{1}{f}\right)_{lab}$$

$$\boxed{n^2 f_{fs} = f_{lab}}$$

Where

n = scale factor

The scaled model calculation can be used if we want to test the prototype in the lab. However, to validate the result, we can use computer simulation technology (CST) software to compare both results.

CHAPTER 3

METHODOLOGY

3.1 Procedure Identification

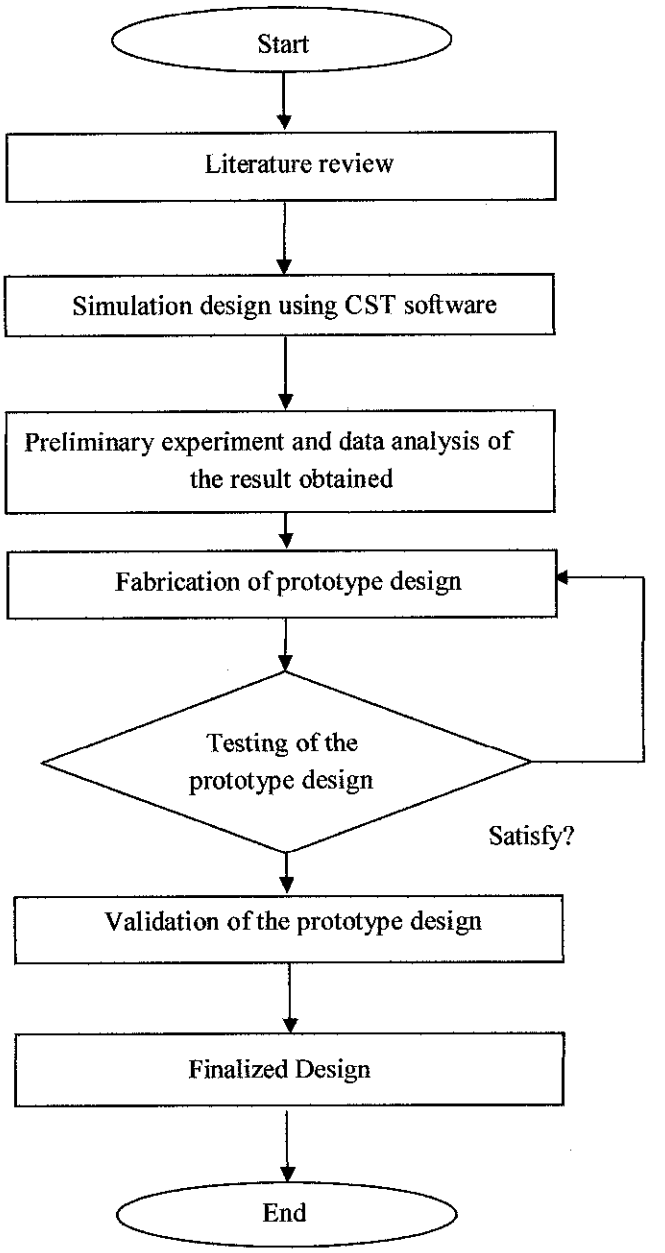

Figure 8: Project flow chart

Upon completing this project, there are several steps involved which can be divided into four main parts:

- Research and literature review
- Simulation design using CST EM Studio
- Fabrication prototype design
- Testing prototype design

The first part of this project begins with the research. Research has been done to get an overview on latest technology that can leads to an improvement in efficiency of Seabed Logging. The topic includes Seismic Technology, Seabed Logging (SBL) and Marine Controlled Source Electromagnetic (CSEM). Other relevant theories and current technology used in hydrocarbon exploration are also reviewed.

Next stage is the design stage by using CST software. Understanding and get familiar with this software is critically important as it is an initial stage to develop the antenna design. There are several criteria need to be consider in the design such as material selection and shape of antenna.

The third stage of this project is fabrication prototype design. From the simulation result, the best basic design of antenna will be chosen to continue with the experimental part. The aimed is to get the powerful enhancement of EM wave.

The final stage is testing the antenna's capability inside the lab. The magnetic field is measured by fluxgate magnetic field sensor. This sensor is then connected to the decaport data acquisition system (DAS) Model NI PXI-1042 for the configuration purposes.

3.2 Technical Design

3.2.1 Computer Simulation Technology (CST) Software

CST EM studio is dedicated to the simulation of static and low frequency devices. It is also the most suitable software that can be used to create simulation design. It enables full 3-dimension (3D) simulation in a wide application range that can be used to simulate various design of the antenna. Various shapes of transmitter design can be created to observe the output results. The results of EM wave can be presented in a form of electrical field, magnetic field, electric flux density and also magnetic field intensity. Therefore, a data analysis can be made in order to select the best design of the antenna.

Various applications in this software can be found which includes actuators, brakes, generators, motors, sensors, switches, transformers measurement and also shielding effect. It provides both orthogonal and tetrahedral meshing in one 3D EM simulator and also three types of solver that can be used in running the simulation which includes electrostatic solver, magnetostatic solver and also full wave solver. The solver which depends on the needs of different sources and the materials must be chosen correctly [41].

3.3 Tools and Equipments of the Experiment

3.3.1 Transmitter

Transmitter is used to generate a useful electromagnetic field at a distance. A transmitter can be made from many types of conductor. Commonly we used copper as the transmitter since it is a highly electricity conductive material. But for this project, aluminum is choose as the material of antenna since it also provides higher electromagnetic wave, light, cheap, easy to fabricate and withstand to the corrosion.

3.3.2 Function Generator

Figure 9: Function generator 5MHz model Instek GFG-8250A

The function generator of brand model Instek GFG-8250A is used to generate EM wave and the minimal frequency of 1 kHz are selected to ensure that the waveform can be transmitted in a long range. Besides that, at frequencies of 1 kHz, the power loss in the internal resistance of the conductor is negligible and all power is either radiated or transferred to the terminations without loss [42].

Square wave is frequently used as transmitter waveform in marine controlled-source electromagnetic or in seabed logging. This type of waveform is easy to generate and it has the advantage of transferring maximum energy to the subsurface of seawater due to the transmitter current is running at its peak amplitude at all times [43]. Without function generator, there is no power supply to the antenna and the EM wave cannot be produced. The output signal can be varied up to the maximum amplitude of 20V peak-to-peak [44].

3.3.3 Decaport Data Acquisition System

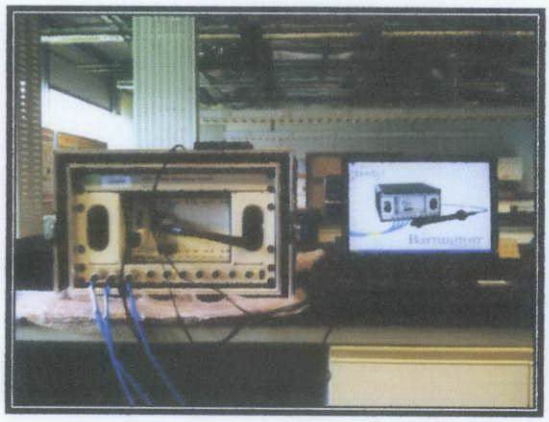

Figure 10: Decaport data acquisition system

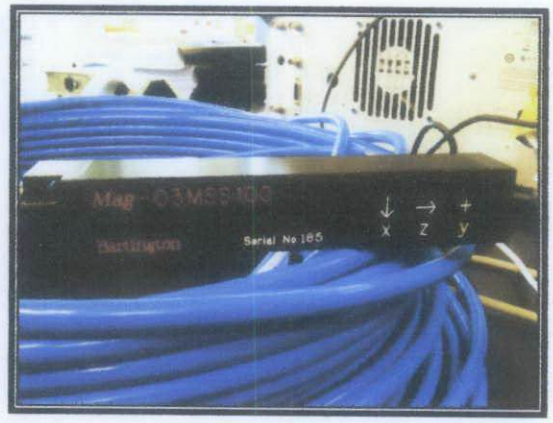

Figure 11: Flux gate magnetic field sensor

The function of the receiver is to detect the received signal and transfer the waveform to the data logger. The same concept is applied to this leading technology system where the magnetic field produced from EM wave can be sensed by fluxgate magnetic field sensor of brand model Mag-03MSS100. This sensor is then connected to the decaport data acquisition system (DAS) Model NI PXI-1042 for the configuration purposes. The fluxgate can detect EM wave in three different directions which is Hx, Hy and Hz [44].

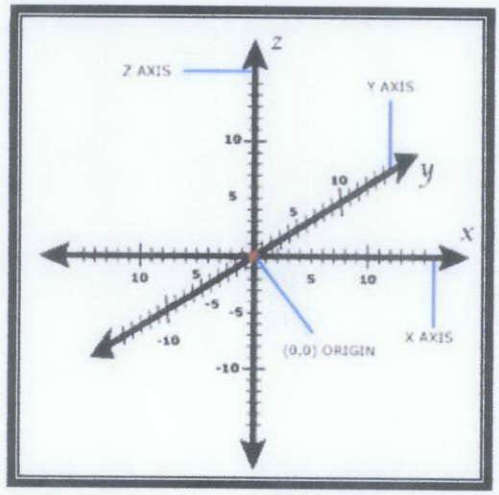

Hx: Move the fluxgate left and right

Hy: Move the fluxgate upward and downward

Hz: Move the fluxgate forward and backward

Figure 12: Three dimensional coordinate system

There are various types of EM sensors but the most popular in the field of hydrocarbon detection are the fluxgate sensor and the squid sensor. The reason these two technologies are mostly applied in this field is because they are highly reliable and efficient in low-field-sensing applications [45].

CHAPTER 4

RESULTS AND DISCUSSION

4.1 Preliminary Experiment

4.1.1 Material Selection

Material selection for the transmitter should be based on the conductivity of a material. The conductivity of a material is a measure of how easily electrons can travel through the material under the influence of an external electric field [28]. It can be defined that the more conductive of the material, the easiest electrons to flow and they can emits the EM wave easily. By refering Table 1, silver shows the highest value of conductivity compared to the others. Although it has higher conductivity, it is still quite expensive. Besides choosing high conductivity, we also need to consider the avaibility of the materials in the lab. As found, only copper and aluminum are available in the lab.

The material for antenna must have high conductivity value. This is because the EM wave strength is depends on current flow. For conducting media, Ohms Law yields the conduction current density $J = \sigma E$

Where σ is the conductivity and E is the electric field. From the equation, we know that the current is proportional to the E field [9].

Even though the copper can generate electromagnetic wave slightly higher than aluminum, other factors need to be taken into consideration such as the cost, and also the ability to withstand to the corrosion under the seawater at high pressure and high temperature condition. . A copper rod is initially being processed from the continuous casting system yield lower tensile strength and lower hardness [46]. Therefore, it can be concluded that aluminum is the best fit to this project design since it has higher resistance corrosion, light, cheaper than copper and also easy to fabricate.

4.1.2 Shape of the Antenna

After we have selected aluminum as the material for the transmitter design, next we want to investigate the shape of the antenna. CST Software is used to determine the basic shape of the antenna. The antenna is designed to two different shape; straight and curve. Below is the setup parameter of the antenna and conditions for simulations:

Table 3: Setup parameter for the simulation

SPECIFICATIONS	DETAILS
Types of material	*Aluminum*
Frequency	0.125Hz
Supply Current	1250A
Diameter (d)	0.1m
Length	270m
Outer Diameter (Curve)	85.94m
Inner Diameter (Curve)	85.84m

Table 4: Conditions for Simulations

SPECIFICATIONS	DETAILS
Air	500m
Seawater	1000m
Overburden	1000m
Oil	100m
Under burden	1000m
Distance of transmitter form seafloor	30m
Offset	10000

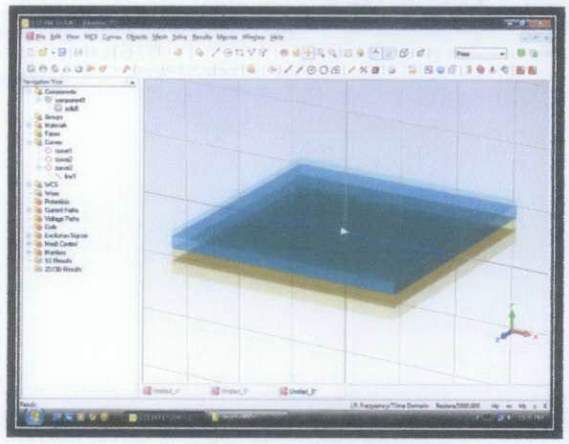

(a) Condition with oil

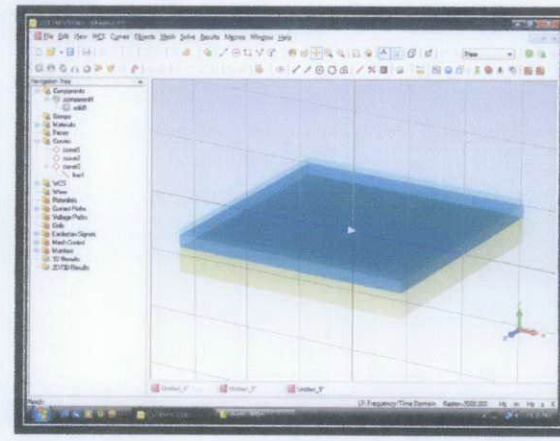

(b) Condition without oil

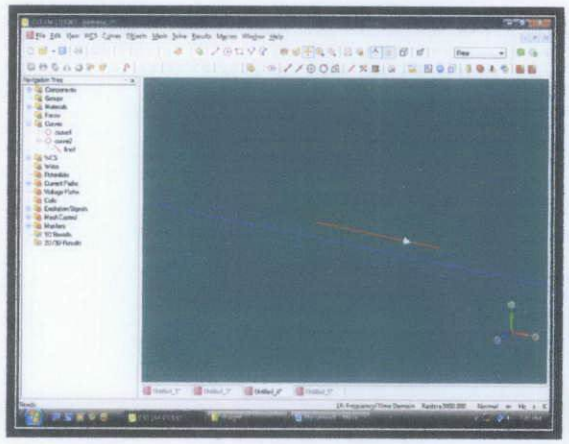

(c) Straight shape

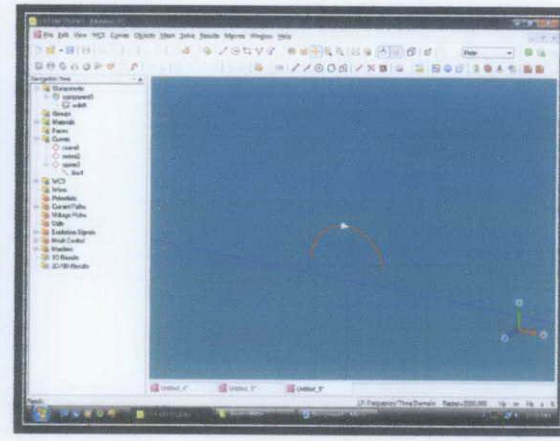

(b) Curve shape

The best shape of antenna is depends on how it can reduce the air wave effect. Thus, for this simulation, we will vary the depth of the sea water by decreasing the depth from 1000m to 100m gradually. Below is the simulation result for two different configurations:

Straight Antenna

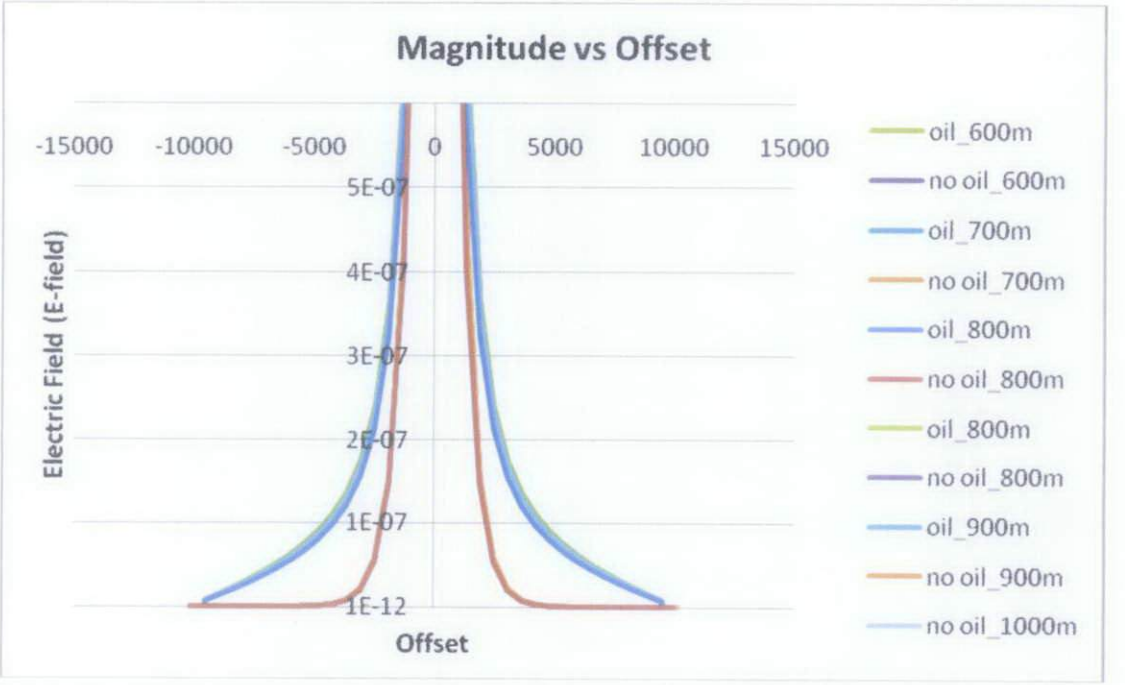

Figure 13: Results for straight antenna with the depth of sea water from 1000m to 600m

From the graph, we can observed that when we decreased the depth of the sea water from 1000m to 600m, the gap between with oil and without oil is getting closer due to the detection of air wave at the detector. The air wave effect has interrupt the reading of the detector. However, the detector still can detect the presence of oil at this range of depth of the sea water.

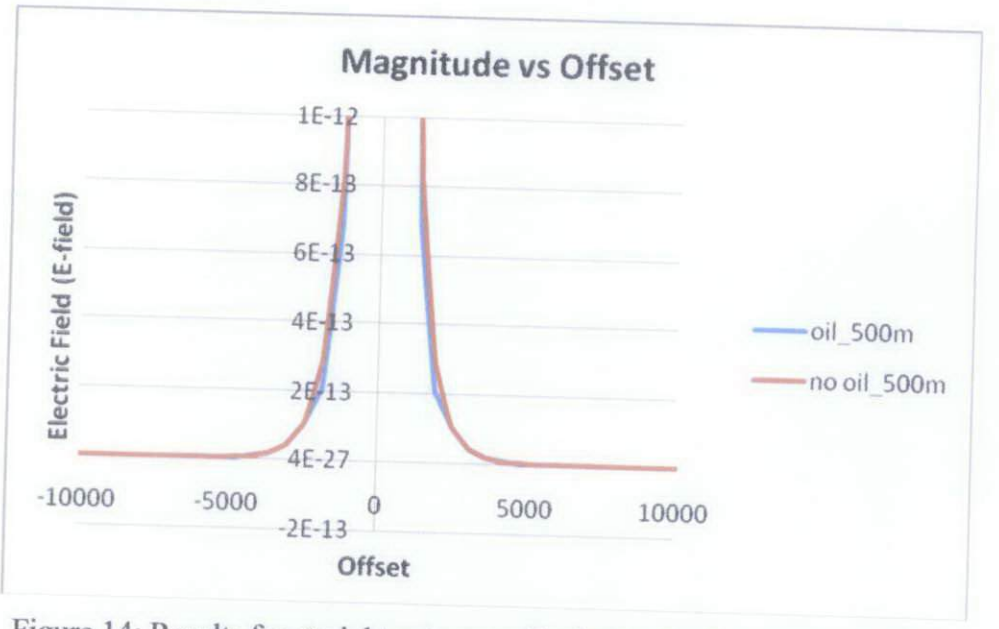

Figure 14: Results for straight antenna with the depth of sea water at 500m

Based on the graph, we can see that the signal from the subsurface had slightly been masked by the unwanted signal of air wave at 500m depth of sea water. The major concern is to ensure that the information obtained from the receivers is the true information about seafloor resistivity rather than the interference.

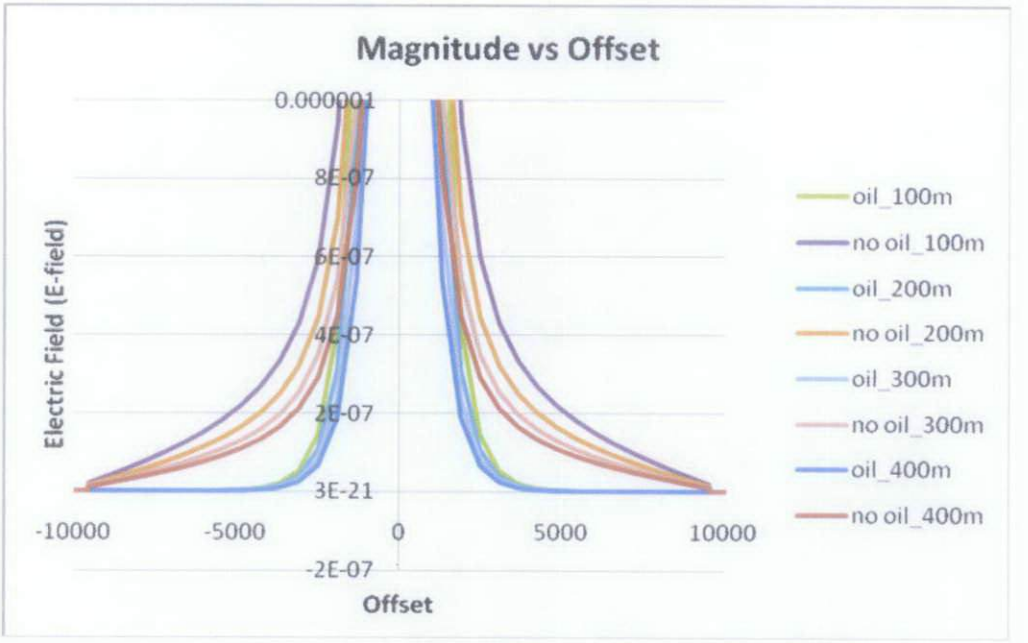

Figure 15: Results for straight antenna with the depth of sea water from 400m to 100m

From the graph above, as we further decreased the depth of the sea water from 400m to 100m, the gap between with oil and without oil are increased. At this depth, the detectors are not be able to detect the presence of oil due to the large effect of air wave. This air wave interferes with the signal that comes from the subsurface and due to this its present is considered as unwanted signal. Air wave effects are notorious in shallow water, where the useful signals from the reservoir or targets might be totally masked by the airwaves which contain little information about subsurface [47].

Table 5: Summary of the straight antenna

Magnitude of E-field at offset 10000m for straight antenna			
Depth of Sea water	Without oil	With oil	% Difference
1000m	9.27E-10	7.52E-08	80.12%
900m	1.01E-09	8.02E-08	78.41%
800m	1.05E-09	8.30E-08	78.05%
700m	1.07E-09	8.34E-08	76.94%
600m	1.17E-09	9.09E-08	76.69%
500m	7.63E-07	7.64E-07	0.13%
400m	1.68E-07	1.00E-08	94.05%
300m	1.93E-07	1.05E-08	94.55%
200m	2.30E-07	1.10E-08	95.22%
100m	2.35E-07	4.31E-09	98.17%

Curve Antenna

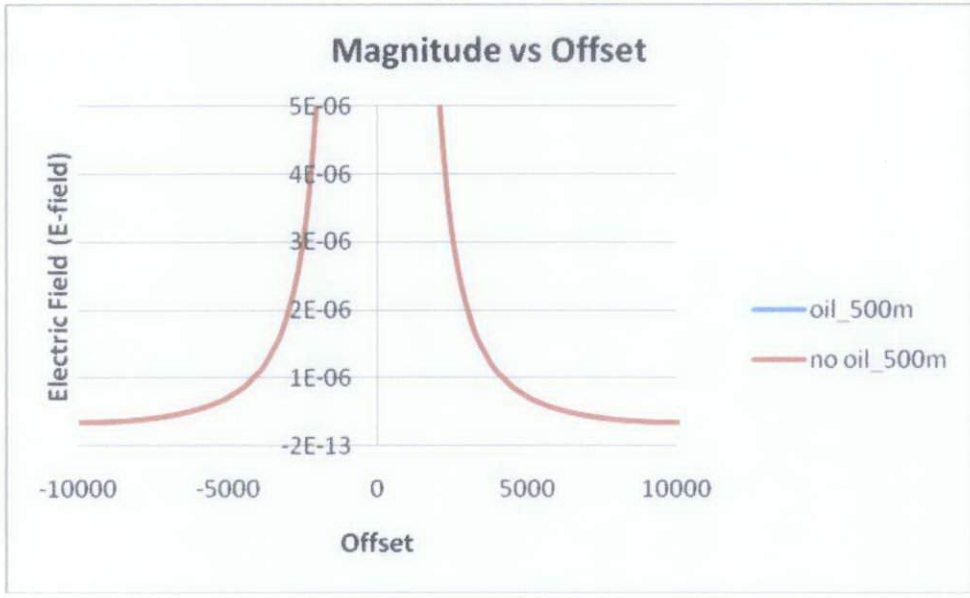

Figure 16: Results for curve antenna with the depth of sea water at 500m

Based on the graph above, we can observe that there is no gap or difference between seabed with oil and without oil. If we compared between straight and curve antenna at the same depth of sea water at 500m, we can see that the curve antenna has successfully reduced the effect of the air wave. However, since the values are the same, the detector still cannot differentiate between the seabed with oil and without oil. An improved of transmitter design is needed in order to solved the problem.

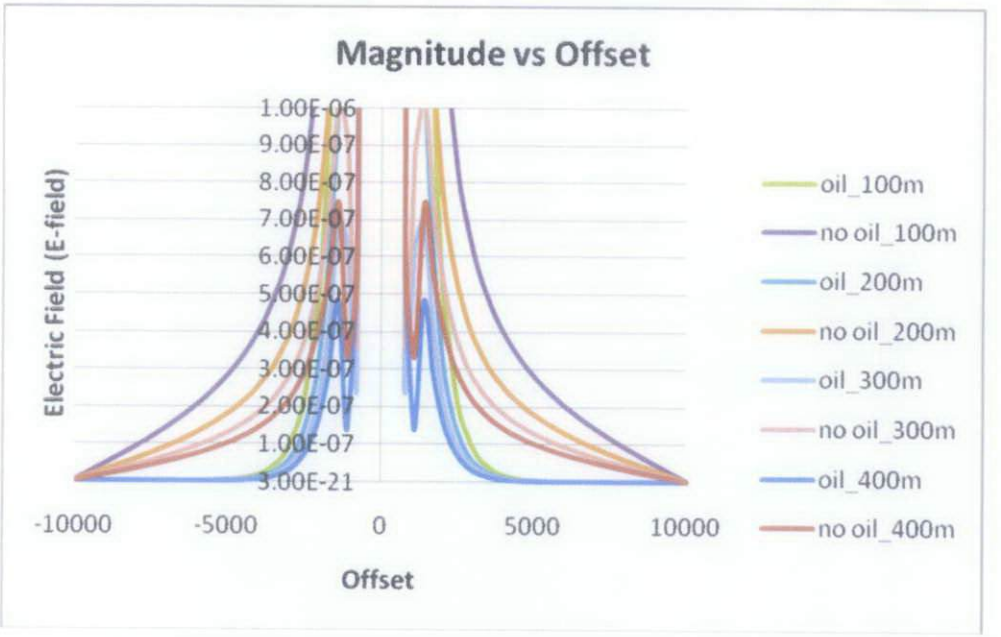

Figure 17: Results for curve antenna with the depth of sea water from 400m to 100m

From the graph, we can see that the gap or difference between seabed with oil and without oil has been reduced if compared to straight antenna at the same depth of sea water. It means that the air wave effect is reduced with the used of the curve antenna. For the curve antenna, the strong signals can be observed due to the higher concentration of electric field at the center of the antenna. This shows that the signal for the curve antenna is more stable and more focused to a particular direction. Thus, it will reduced the effect of the air wave and be able to emits strong electromagnetic wave.

Table 6: Summary of the curve antenna

Magnitude of E-field at offset 10000m for curve antenna			
Depth of Sea water	Without oil	With oil	% Difference
500m	1.13E-06	1.13E-06	0%
400m	3.27E-07	9.66E-08	70.46%
300m	3.43E-07	7.49E-08	78.16%
200m	3.45E-07	3.73E-08	89.19%
100m	4.96E-07	4.26E-08	91.41%

4.1.3 Scaled Factor

For the scaled model to be an accurate representation of the full size system, the parameters that describe it must satisfy definition relations that are determined by the chosen scaled factor [48]. The calculation is based on the equation in Chapter 2 – Literature Review, and the results as shown in Table 7, Table 8 and Table 9.

Table 7: Scaled Calculation for 1000 Scale Factor

Scale Factor, n	Frequency, f (Hz)		Wavelength, λ (m)		Transmitter length, l (m)		Skin depth, δ (m)	
	$f_{full\ scale}$	$f_{lab\ scale}$	$\lambda_{full\ scale}$	$\lambda_{lab\ scale}$	$l_{full\ scale}$	$l_{lab\ scale}$	$\delta_{full\ scale}$	$\delta_{lab\ scale}$
1000	1.0000	1000000	1732.14	1.732	433.035	0.433	275.678	0.276
	0.5000	500000	2449.61	2.450	612.403	0.612	389.868	0.390
	0.2500	250000	3464.27	3.464	866.068	0.866	551.357	0.551
	0.1250	125000	4899.22	4.899	1224.805	1.225	779.739	0.780
	0.0625	62500	6928.55	6.929	1732.138	1.732	1102.713	1.103

Table 8: Scaled Calculation for 2000 Scale Factor

Scale Factor, n	Frequency, f (Hz)		Wavelength, λ (m)		Transmitter length, l (m)		Skin depth, δ (m)	
	$f_{full\ scale}$	$f_{lab\ scale}$	$\lambda_{full\ scale}$	$\lambda_{lab\ scale}$	$l_{full\ scale}$	$l_{lab\ scale}$	$\delta_{full\ scale}$	$\delta_{lab\ scale}$
2000	1.0000	4000000	1732.14	0.866	433.035	0.217	275.678	0.138
	0.5000	2000000	2449.61	1.225	612.403	0.306	389.868	0.195
	0.2500	1000000	3464.27	1.732	866.068	0.433	551.357	0.276
	0.1250	500000	4899.22	2.450	1224.805	0.612	779.739	0.390
	0.0625	250000	6928.55	3.464	1732.138	0.866	1102.713	0.551

Table 9: Scaled Calculation for 3000 Scale Factor

Scale Factor, n	Frequency, f (Hz)		Wavelength, λ (m)		Transmitter length, l (m)		Skin depth, δ (m)	
	$f_{full\ scale}$	$f_{lab\ scale}$	$\lambda_{full\ scale}$	$\lambda_{lab\ scale}$	$l_{full\ scale}$	$l_{lab\ scale}$	$\delta_{full\ scale}$	$\delta_{lab\ scale}$
3000	1.0000	9000000	1732.14	0.577	433.035	0.144	275.678	0.092
	0.5000	4500000	2449.61	0.817	612.403	0.204	389.868	0.130
	0.2500	2250000	3464.27	1.155	866.068	0.289	551.357	0.184
	0.1250	1125000	4899.22	1.633	1224.805	0.408	779.739	0.260
	0.0625	562500	6928.55	2.31	1732.138	0.577	1102.713	0.368

The red box indicates the parameters that will be chosen to conduct the experiment. The radius of the transmitter can be easily calculated from the transmitter length.

4.1.4 Prototype Design and Construction

It should be recalled from previous simulation that the curve transmitter had resulted to the highest magnification of the EM waves. This work promise deals with studying the effect of curvature on the magnification of the EM waves. Thus, curve antenna will be chosen as a basic transmitter design for this project.

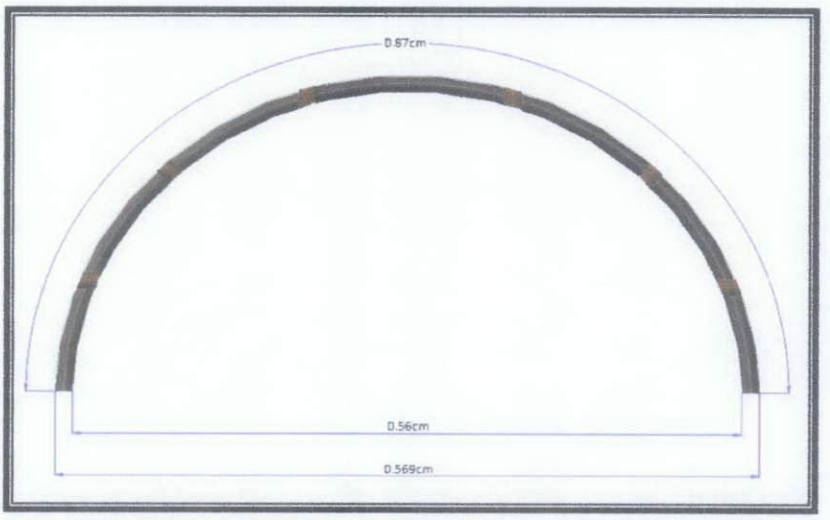

Figure 18: Schematic Diagram of Curve Transmitter

From this basic curve transmitter design, an improved transmitter with four combination of curve transmitter has been fabricated. For the Quadrapole antenna, the design is originated from the four curves of aluminum rods which are centered in the middle.

Figure 19: Quadrapole Antenna

4.2 Experiment 1: Effect of Magnetic Field Strength over the Distance

In this experiment, the objective is to demonstrate the effect of magnetic field strength over the distance. Vary the distance from r' distance (28cm) and double position from the first one which is equivalent to the '2r' distance (56cm). The distance will keep on increasing gradually. An illustration to this setup experiment is shown at figure below.

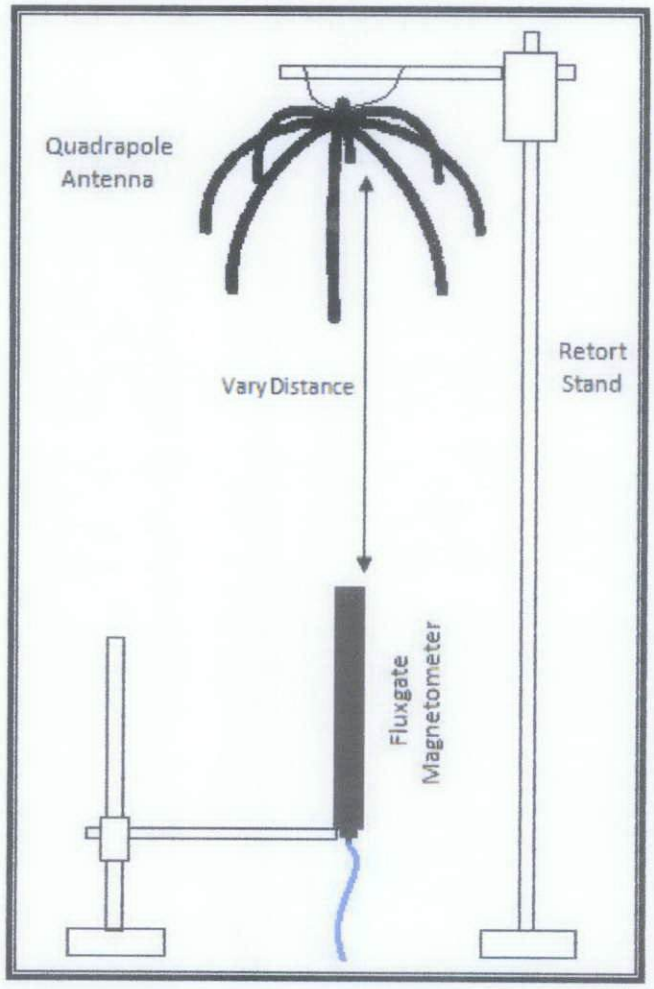

Figure 20: Schematic Diagram of the Experimental Setup

There will be three different wiring connections; parallel, series and parallel to parallel. And for each of these wiring connections, the feeding points are placed at two different points; at the center and at the end of each curve antenna. See table below.

Table 10: Six Different Configuration Setup

Configuration	Connection	Feeding Points
1	Parallel	At the center
	Parallel	At the end
2	Series	At the center
	Series	At the end
3	Parallel to Parallel	At the center
	Parallel to Parallel	At the end

4.2.1 Parallel Connection

For the ***first configuration***, each curve transmitter will be connected to one function generator. See figure below.

Connection 1:

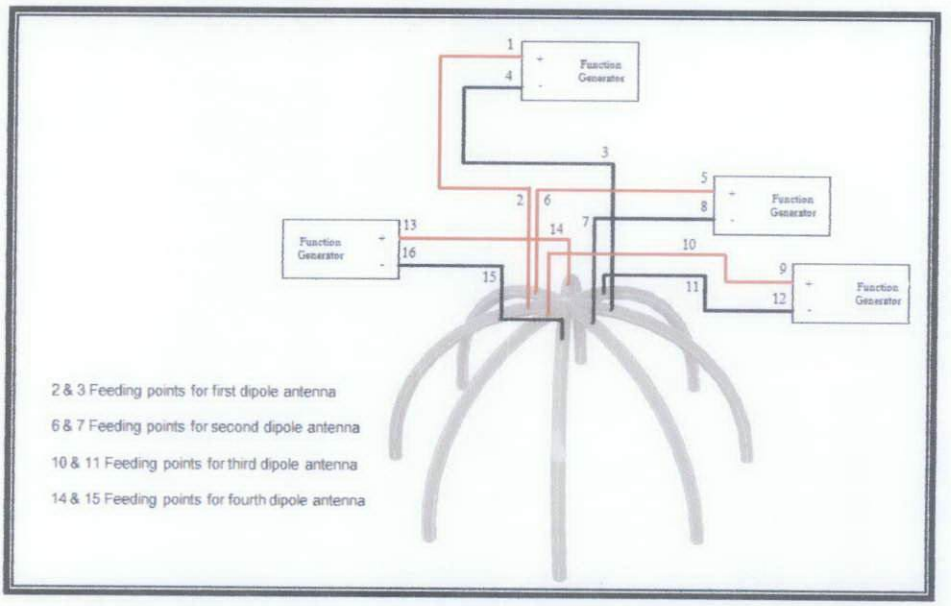

Figure 21: Quadrapole Antenna in parallel with Feeding Points at the center

Connection 2:

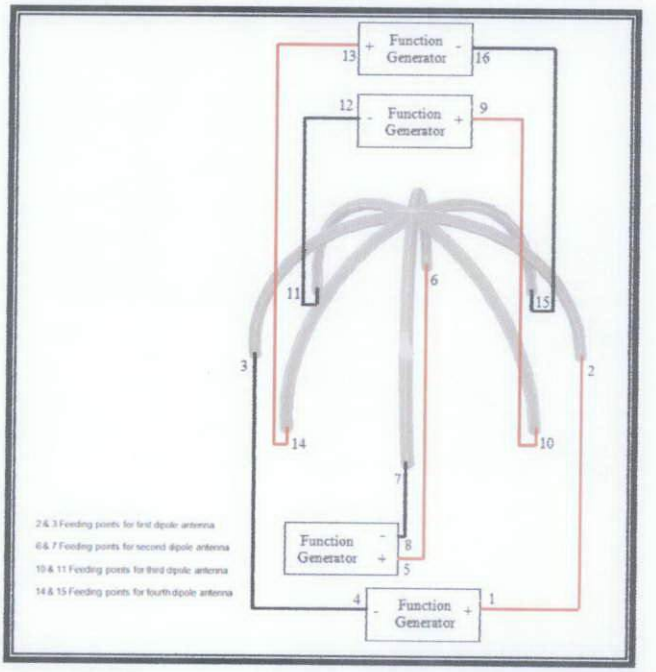

Figure 22: Quadrapole Antenna in parallel with Feeding Points at the end

The results for configuration 1 are tabulated in Table 10.

Table 11: Result of configuration 1

Distance	Connection 1	Connection 2
28cm	1.77E-07	6.45E-08
56cm	7.87E-08	2.45E-08
84cm	2.17E-08	1.29E-08
112cm	1.67E-08	8.01E-09
140cm	1.01E-08	5.42E-09
168cm	3.81E-09	4.03E-09
196cm	3.13E-09	3.39E-09
224cm	2.67E-09	2.87E-09
252cm	2.58E-09	2.39E-09
280cm	2.30E-09	1.99E-09
308cm	2.04E-09	1.80E-09
336cm	1.88E-09	1.74E-09
364cm	1.86E-09	1.67E-09
392cm	1.80E-09	1.64E-09
420cm	1.75E-09	1.43E-09
448cm	1.70E-09	1.43E-09
476cm	1.66E-09	1.43E-09
504cm	1.64E-09	1.43E-09
532cm	1.44E-09	1.43E-09
560cm	1.44E-09	1.43E-09

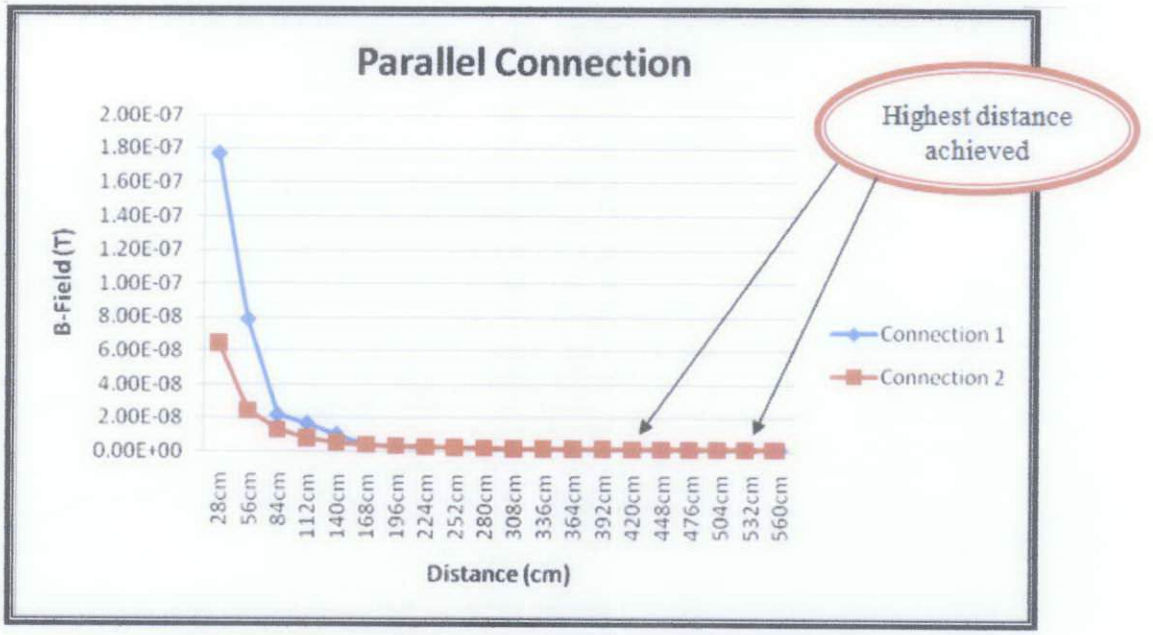

Figure 23: Graph of configuration 1

Based on the result, the magnetic field detected by the detector started to constant when it reached its limit. It shows that the antenna can only transmit up to a certain distance. When the antenna is connected as in connection 1, it can transmit the signal up to 5.32m of distance with a percentage different of 196.77%. As for connection 2, the antenna can transmit the signal up to 4.20m with a percentage difference of 191.32%. The position of the feeding point actually affects the results. When the feeding points are place at the center, high concentration of electric field is produced at the center of the antenna. Thus, strong EM wave can be transmitting by the antenna.

4.2.2 Series Connection

For the ***second configuration***, the connection is in series with all curves connected to one function generator. See figure below.

Connection 3:

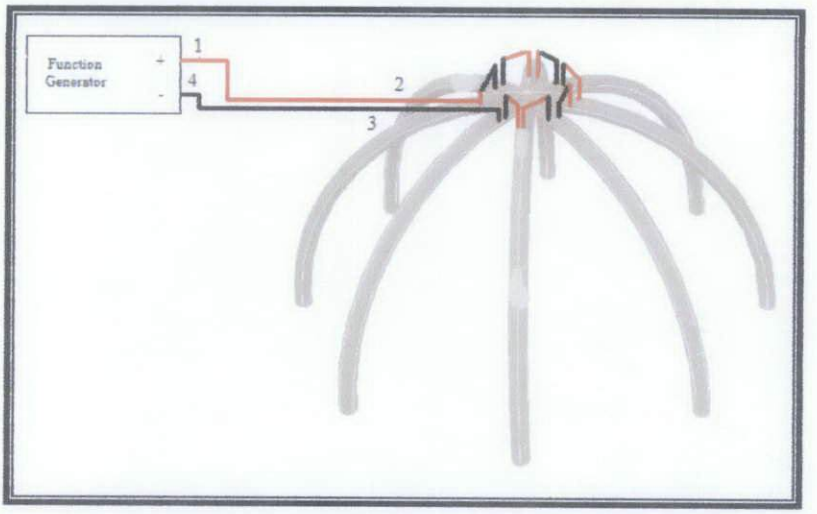

Figure 24: Quadrapole Antenna in series with Feeding Points at the center

Connection 4:

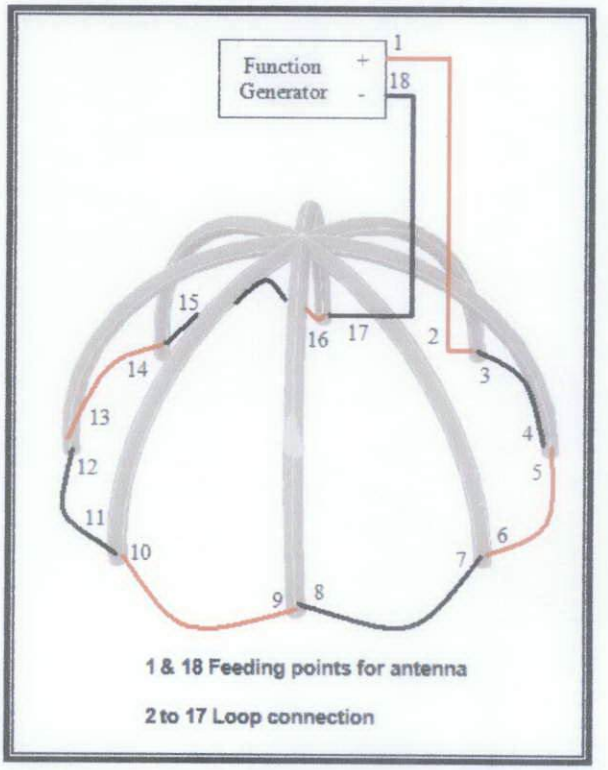

Figure 25: Quadrapole Antenna in series with Feeding Points at the end

The results for configuration 2 are tabulated in Table 12.

Table 12: Result of configuration 2

Distance	Connection 3	Connection 4
28cm	6.96E-09	3.14E-09
56cm	2.97E-09	1.88E-09
84cm	2.67E-09	1.55E-09
112cm	2.28E-09	1.46E-09
140cm	1.97E-09	1.46E-09
168cm	1.67E-09	1.46E-09
196cm	1.45E-09	1.46E-09
224cm	1.45E-09	1.46E-09

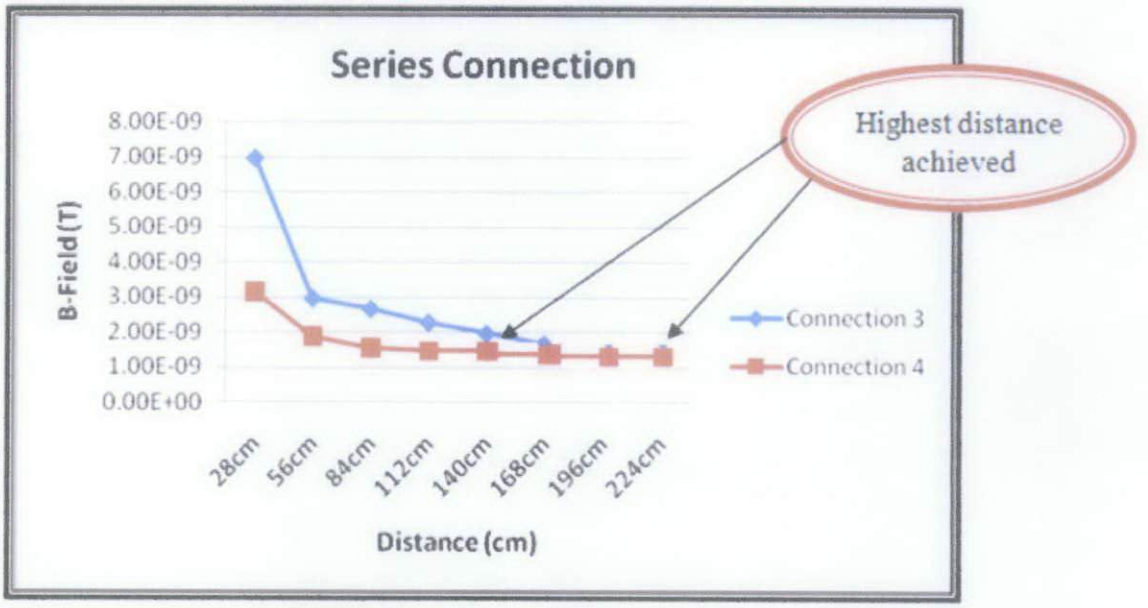

Figure 26: Graph of configuration 2

From the result, we can observe that when the distance between the antenna and detector is increased, the output of magnetic field received at detector is decreased. The signal wave attenuation is proportional to the distance due to losses caused by ohmic resistive losses in the conductive earth and to the dielectric properties of the earth [41]. These losses are happen during the propagation of signal wave. According to Biot-Savart Law equation:

$$\vec{B} = \hat{\phi}\frac{\mu_0 I}{2\pi r} \tag{8}$$

We can see the relationship between magnetic flux density B with distance r is inversely proportional to each other.

Besides, from the graph we can observe that the highest distance achieved for connection 3 is 1.96m with a percentage difference of 131.03% which is slightly higher than connection 4 which is 1.40m and the percentage difference of 73.04%. It should be recalled from the previous parallel connection, if the feeding points are placed at the center, it yields to a better result. Same goes for this type of connection. However, if we compared between the series and parallel connection, it is clear that parallel connection can transmit the signal at a far distance than the series connection because the used of four function generator compared to series connection which only used one function generation as a power supply. Besides, in a series circuit, the current through each of the components is the same while in a parallel circuit, the total current is the sum of the currents through each component [49]. Therefore, parallel connection gives better result due to the amount of current received by the transmitter.

4.2.3 Parallel to Parallel Connection

For the ***third configuration***, the connection is in parallel to parallel. Two curves will connected in parallel and the parallel connection will be connected to one function generator. See figure below.

Connection 5:

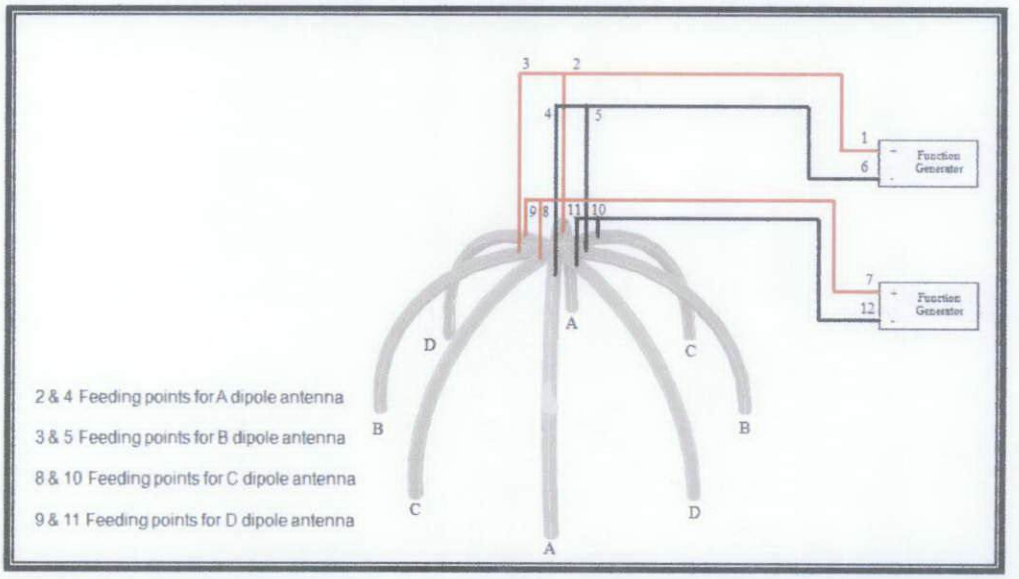

Figure 27: Quadrapole Antenna in parallel to parallel with Feeding Points at the center

Connection 6:

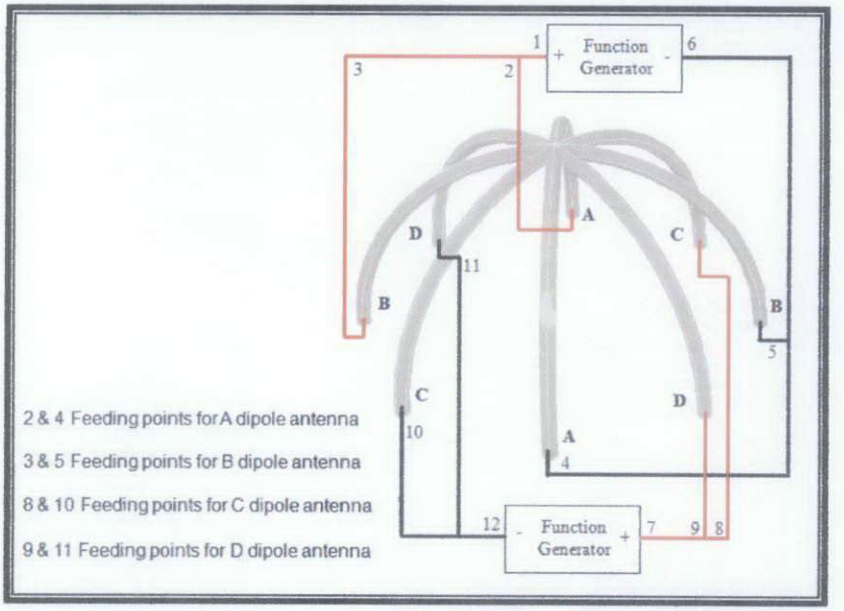

Figure 28: Quadrapole Antenna in parallel to parallel with Feeding Points at the end

The connection for parallel to parallel can be in 4 different connections. See table below.

Table 13: Parallel to parallel connection

Connection	W	X	Y	Z
Function Generator 1	A/B	B/C	C/D	A/D
Function Generator 2	C/D	A/D	A/B	B/C

From the table above, for connection W, two curves A/B will be connected parallel to Function Generator 1 while another two curves C/D is connected to Function Generator 2. If in connection X, B/C connected to Function Generator 1 and A/D to Function Generator 2. Same goes to the other two connections.

The results for configuration 3 are tabulated in Table 14 and Table 15.

Table 14: Result of configuration 3 for the connection 5

Distance	B-Field (T) at connection W	B-Field (T) at connection X	B-Field (T) at connection Y	B-Field (T) at connection Z
28cm	4.29E-08	3.78E-08	4.14E-08	4.42E-08
56cm	5.36E-08	5.26E-08	5.32E-08	5.26E-08
84cm	7.24E-09	6.53E-09	7.51E-09	6.22E-09
112cm	5.46E-09	3.78E-09	5.27E-09	5.35E-09
140cm	3.25E-09	3.17E-09	3.19E-09	4.21E-09
168cm	3.12E-09	3.05E-09	3.09E-09	3.15E-09
196cm	2.76E-09	2.65E-09	2.79E-09	2.61E-09
224cm	2.38E-09	2.45E-09	2.33E-09	2.38E-09
252cm	2.13E-09	2.21E-09	2.17E-09	2.16E-09
280cm	1.87E-09	1.82E-09	1.91E-09	1.94E-09
308cm	1.76E-09	1.72E-09	1.70E-09	1.73E-09
336cm	1.68E-09	1.69E-09	1.68E-09	1.68E-09
364cm	1.66E-09	1.62E-09	1.66E-09	1.63E-09
392cm	1.56E-09	1.58E-09	1.59E-09	1.56E-09
420cm	1.43E-09	1.46E-09	1.44E-09	1.43E-09
448cm	1.43E-09	1.46E-09	1.44E-09	1.43E-09

Table 15: Result of configuration 3 for the connection 6

Distance	B-Field (T) at connection W	B-Field (T) at connection X	B-Field (T) at connection Y	B-Field (T) at connection Z
28cm	2.74E-08	2.66E-08	2.71E-08	2.61E-08
56cm	1.03E-08	1.12E-08	1.18E-08	1.06E-08
84cm	6.44E-09	6.30E-09	6.37E-09	6.51E-09
112cm	4.51E-09	4.58E-09	4.48E-09	4.46E-09
140cm	3.64E-09	3.56E-09	3.49E-09	3.66E-09
168cm	3.02E-09	3.05E-09	3.08E-09	3.01E-09
196cm	2.54E-09	2.53E-09	2.66E-09	2.51E-09
224cm	2.22E-09	2.26E-09	2.29E-09	2.21E-09
252cm	2.01E-09	2.05E-09	2.11E-09	2.08E-09
280cm	1.82E-09	1.82E-09	1.84E-09	1.82E-09
308cm	1.76E-09	1.70E-09	1.76E-09	1.73E-09
336cm	1.46E-09	1.43E-09	1.47E-09	1.43E-09
364cm	1.46E-09	1.43E-09	1.47E-09	1.43E-09
392cm	1.46E-09	1.43E-09	1.47E-09	1.43E-09
420cm	1.46E-09	1.43E-09	1.47E-09	1.43E-09
448cm	1.46E-09	1.43E-09	1.47E-09	1.43E-09

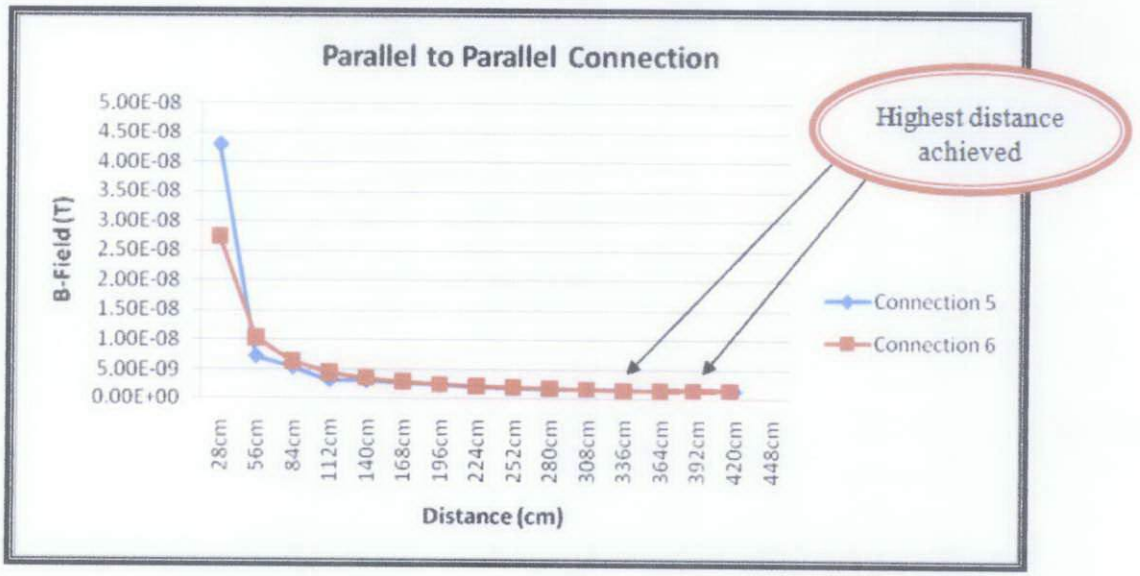

Figure 29: Graph of configuration 3

From the result, we can see that if we choose to connect the antenna in parallel to parallel connection, all connections W, X, Y and Z are acceptable as it yield to almost a similar result. However, connection 5 gives a better result with a percentage difference of 187.10% where the antenna can transmit the signal until 3.92m compared to connection 6 with a percentage difference of 179.76% which is only 3.36m. Once again, the position of the feeding points plays an important role. Thus, connection 5 is better than connection 6.

After testing the antenna with three different configurations, we can observe that the parallel connection with feeding points at the center can transmit the EM wave at the highest distance.

Table 16: Summary of the different connection

CONFIGURATION	DETAILS	% DIFFERENCE
1	Parallel + Feeding Points at the center	196.77%
2	Parallel + Feeding Points at the end	191.32%
3	Series + Feeding Points at the center	131.03%
4	Series + Feeding Points at the end	73.04%
5	Parallel to Parallel + Feeding Points at the center	187.10%
6	Parallel to Parallel + Feeding Points at the end	179.76%

By referring to the table above, parallel connection with feeding points at the center gives highest percentage difference compared to the other connection. Thus, this connection will be used to conduct the next experiments.

4.3 Experiment 2: Effect of Different Position of Detector

The next experiment is to determine the best position of detector that can gives highest possible value of magnetic field generated from the Quadrapole antenna. It has to be recalled from the previous experiment that among three configurations, parallel connection with feeding points at the center gives tremendous result. Thus, this type of connection will be used to conduct this experiment.

For this experiment, there are two configurations in placing the detector ; moves the detector left and right and moves the detector all around the antenna for four different position. The distance is fixed at 'r' distance which is equivalent to 28cm.

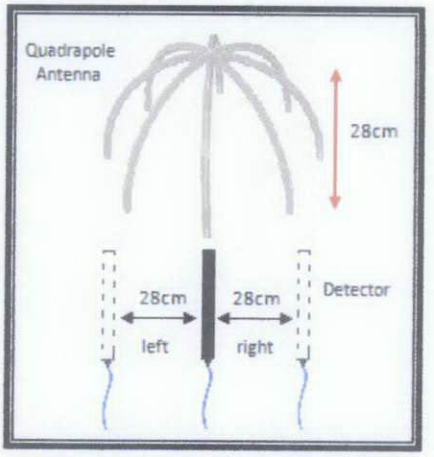

Figure 30: Experimental Setup for Configuration 1

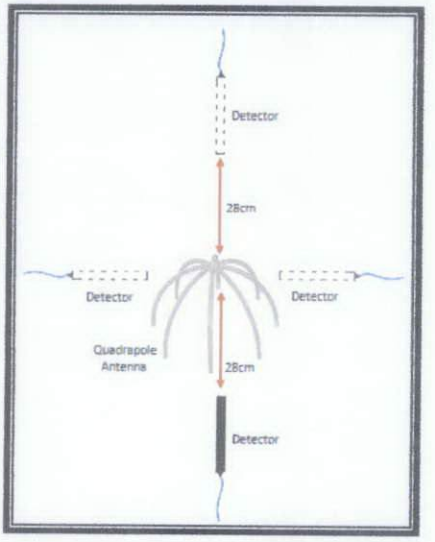

Figure 31: Experimental Setup for Configuration 2

Table 17: Result of configuration 1 with an illustration of setup diagram

POSITION	SETUP DIAGRAM	B-FIELD (Vs/m^2) DETECTED
1	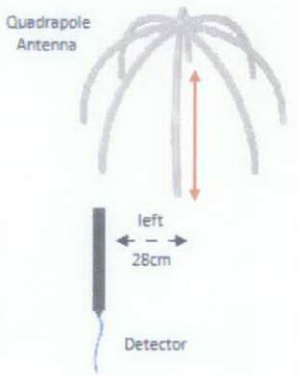	6.42×10^{-09}
2	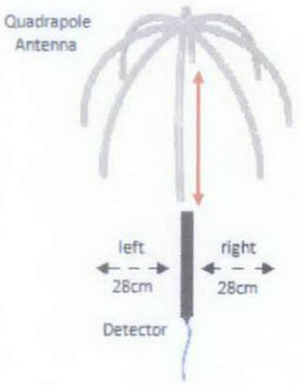	1.77×10^{-07}
3	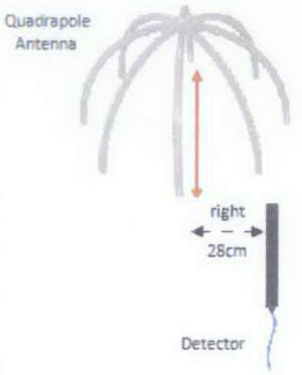	6.48×10^{-09}

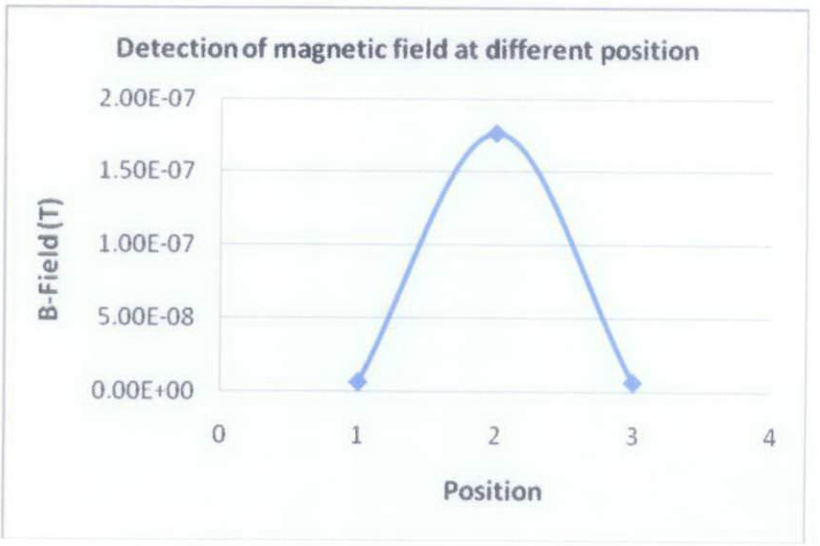

Figure 32: Graph Result of Configuration 1 for Experiment 2

Based on the graph, we can see that a highest value of B-Field is achieved when the detector is placed at the center position. However, the output signal has been reduced when the detector is placed at both end of Quadrapole antenna. Basically, we fed the injected current at the center of the antenna. Hence, there is more flux density and higher concentrating of the magnetic field at the center as shown in Figure 32.

The results for configuration 2 are tabulated in Table 18.

Table 18: Result of configuration 2 with an illustration of setup diagram

POSITION	SETUP DIAGRAM	B-FIELD (Vs/m^2) DETECTED
1	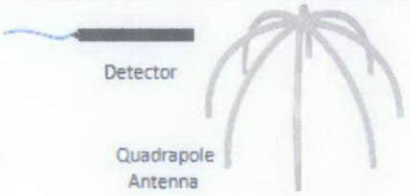	1.85×10^{-08}
2	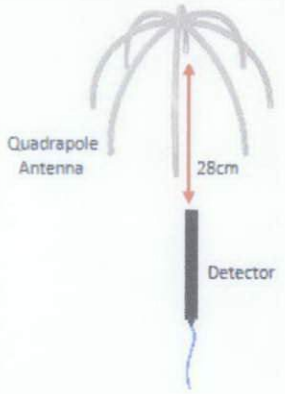	1.77×10^{-07}
3	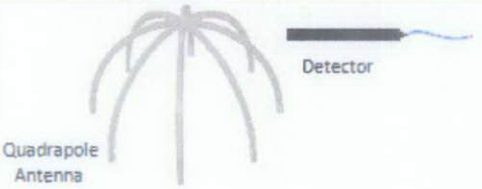	1.47×10^{-08}
4	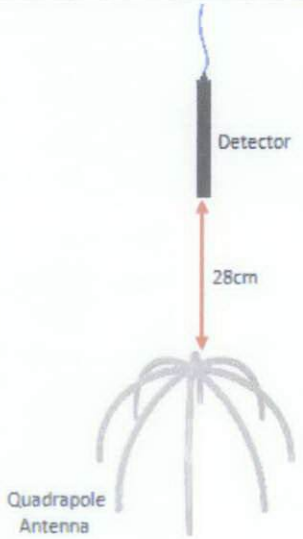	2.07×10^{-08}

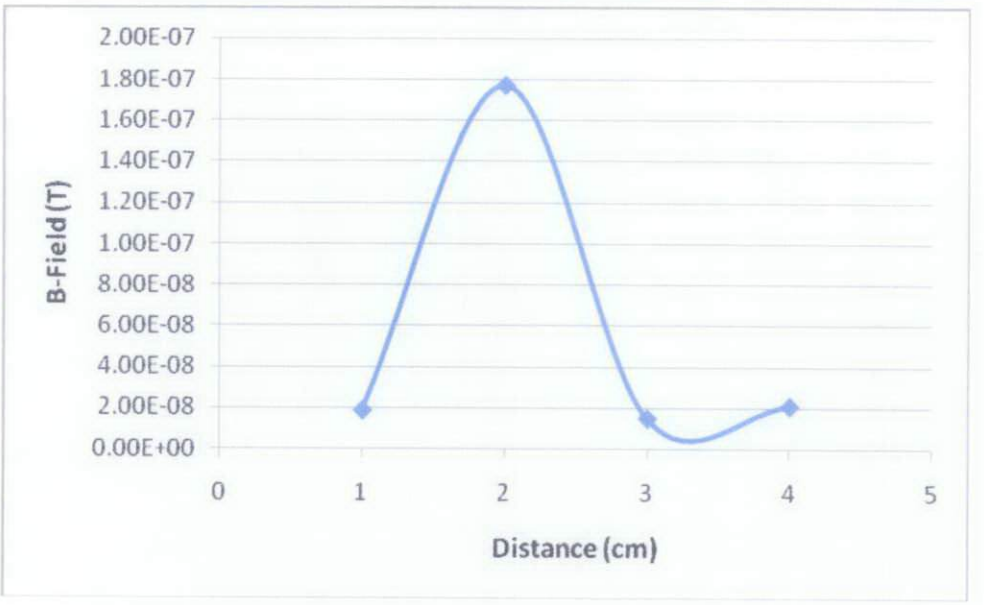

Figure 33: Result of Configuration 2 for Experiment 2

From the plotted graph, we can observe that a highest value of B-Field is achieved when the detector is placed at the center position. The magnetic field can still be detected if we placed at other position. However, the output signal is not as high as when we placed at the center position. The shape of the Quadrapole antenna has the directivity which is the ability of an antenna to focus energy in a particular direction when transmitting the signal. The directivity measures how much more intensely the antenna radiates in its preferred direction [50]. Thus, most of high concentrated of EM wave are from the curve down of the antenna.

4.4 Experiment 3: Effect of Different Turn of Copper Windings on Magnetic Feeders

For this experiment, we vary the number of winding on magnetic feeders. The objective of this experiment is to demonstrate the effect of different turn of copper windings on magnetic feeders. The distance between antenna and detector is fixed to 100cm. Only the number of winding on magnetic feeders will increased gradually from 5 turns to 30 turns.

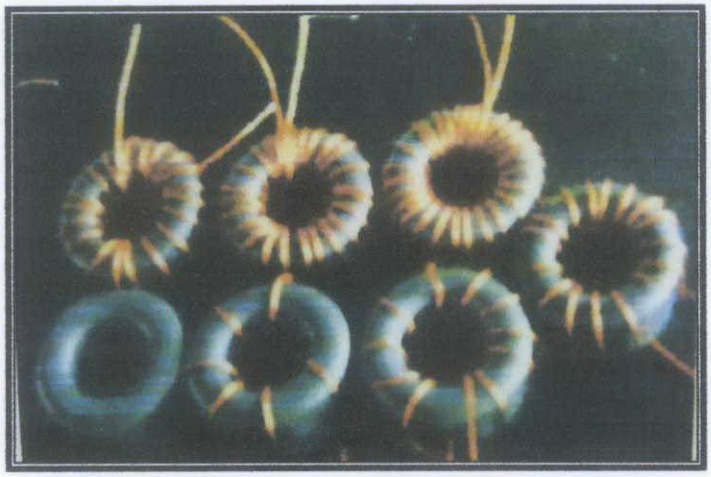

Figure 34: Magnetic Feeders with different turn of copper winding

Here we used ferrite plate with copper winding as a detector which is connected to the oscilloscope.

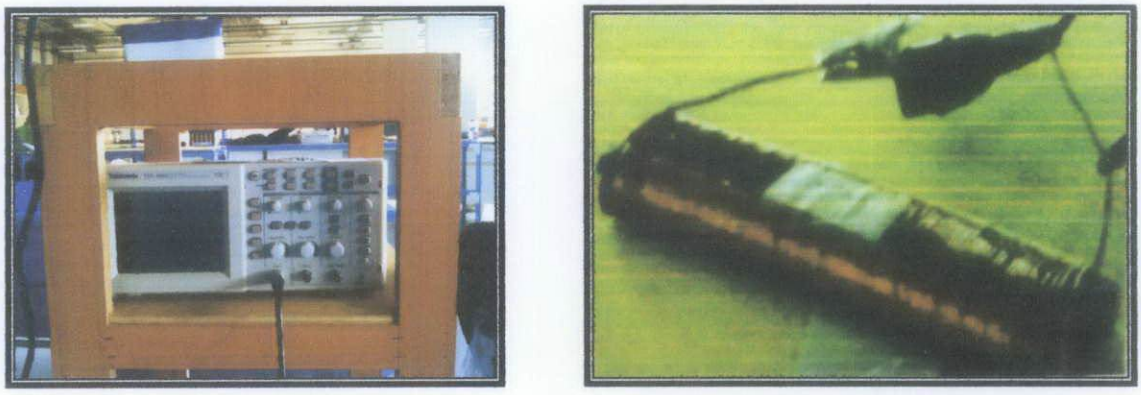

Figure 35: Detector with oscilloscope (left) and ferrite plate with copper winding as detector

The requirements of the detector are given in the table below:

Table 19: Detector requirement for experiment 3

Detector	
Type	Plate
Core	Ferrite plate with copper winding
Length	0.098m
Thickness	0.006m
Number of copper winding	100
Copper winding diameter	0.0008m

The graph of output voltage was observed and the voltage value at the detector is in table below:

Table 20: Result for experiment 3

Number of winding	Output Voltage, V_{p-p} (mV)	Output frequency, f (Hz)
5	57.9	4.961M
10	51.3	16.56M
15	45.8	15.31M
20	74.3	4.673M
25	63.9	16.62M
30	48.1	15.04M

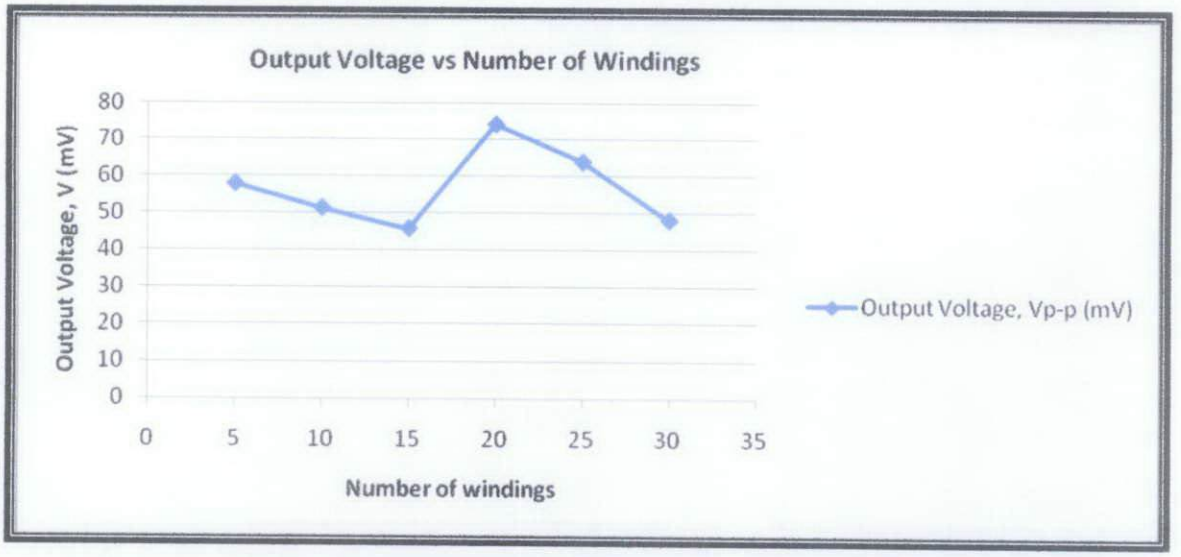

Figure 36: Graph of output voltage vs. number of windings on magnetic feeders

From the result, it shows that the ideal number of windings for the magnetic feeders is 20 turns. There are several factors when making toroid transformer which are toroid size, core material and number of turns of wire. The toroid size and frequency range are selected and the only left to vary is the number of turns [51]. Thus, 20 turns of windings on magnetic feeders will be used for the next experiment.

4.5 Experiment 4: Prototype Testing

The objective of this experiment is to prove that the prototype can transmit a strong signal with magnetic feeders as a secondary tools to enhance the induced of magnetic field. Magnetic feeders also known as toroidal core is a doughnut-shaped structure with closely spaced turns of wire wrapped around it.

Figure 37: Prototype testing

The requirements of the Quadrapole antenna, magnetic feeders and power supply are given in the table below:

Table 21: Antenna requirement for prototype testing

Quadrapole Antenna	
Material	Aluminum
Shape	Quadrapole
Length, L	0.87cm for each curve
Diameter, d	0.56m
Magnetic Feeders	
Code	D28
Material	Nickel Zinc Ferrites
Shape	Toroid

Number of feeders	8 feeders
Inner diameter	0.0195m
Outer diameter	0.0370m
Height	0.0200m
Number of copper winding	20
Copper winding diameter	0.0008m
Power Supply	
Model	Instek GFG-8250A
Frequency	5MHz
Waveform type	Square

For final testing of the prototype, we used parallel connection with feeding points at the center. Magnetic feeders are placed next to each feeding points which connected in series with current sources. The schematic diagram of antenna configuration:

The distance between antenna and detector is varied and the magnetic field detected is in table below.

Table 22: Result for prototype testing

Distance (cm)	B-Field (T)
28cm	9.66E-07
56cm	7.54E-07
84cm	6.56E-07
112cm	4.69E-07
140cm	2.15E-07
168cm	9.26E-08
196cm	8.78E-08
224cm	8.67E-08
252cm	8.18E-08
280cm	7.94E-08
308cm	7.58E-08
336cm	7.22E-08
364cm	7.16E-08

392cm	6.98E-08
420cm	6.72E-08
448cm	5.32E-08
476cm	5.21E-08
504cm	4.91E-08
532cm	4.89E-08
560cm	2.98E-08
588cm	2.15E-08
616cm	8.73E-09
644cm	8.56E-09
672cm	7.61E-09
700cm	6.89E-09
728cm	6.17E-09
756cm	5.76E-09
784cm	5.12E-09
812cm	4.87E-09
840cm	4.43E-09
868cm	3.76E-09
896cm	3.25E-09
924cm	3.01E-09
952cm	2.96E-09
980cm	2.57E-09
1008cm	2.44E-09
1036cm	2.07E-09
1064cm	1.78E-09
1092cm	1.66E-09
1120cm	1.63E-09
1148cm	1.53E-09
1176cm	1.52E-09
1204cm	1.49E-09
1232cm	1.44E-09
1260cm	1.44E-09

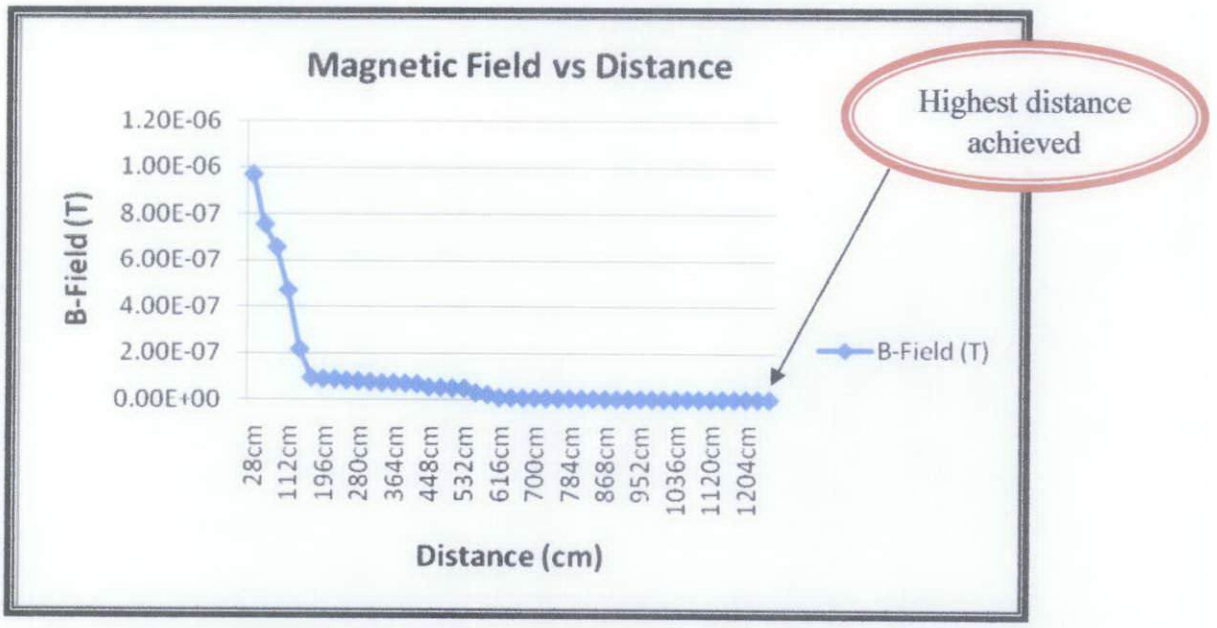

Figure 38: Graph of prototype testing

From the graph, it shows that the magnetic field value starts to decrease as we increased the distance. However, the antenna can transmit the EM wave up to 12m with a percentage diference of 199.33% because of the presence of magnetic feeders. When we supply current through wire winding, magnetic field, H is enclosed in the toroid body. Since magnetic field is always perpendicular to the electric field, the electric field is concentrated at the centre of the toroid. When the dipoles are placed in the concentrated electric field, a high amount of current will flow in the dipole [52]. See figure below.

Figure 39: Toroidal coil with wire windings [53]

CHAPTER 5

CONCLUSION AND RECOMMENDATIONS

5.1 Conclusion

The development of Quadrapole Antenna for hydrocarbon exploration has increase the performance of the electromagnetic wave transmitted from the antenna. The experiments has successfully fulfill the objectives which are to design and to construct a Quadrapole Antenna to demonstrate the effect of magnetic feeders and to provide a prototype that can transmit the strong EM signal. The EM wave consists of electric field and magnetic field which are perpendicular to each other. Since the SBL approach is using EM wave, related theory such as EM wave, Biot-Savart Law, Lenz Law are very useful in order to understand the concept very well. The results from the experiments had shown impressive output readings. Before modeling the prototype of the Quadrapole Antenna, it is very important to do the material selection and design the suitable shape of the antenna that fulfills the objectives. Two basic shape of the antenna is designed by using CST software. Among the two basic designs which are straight and curve, it shows that curve antenna can reduce the effect of air wave that interfere the actual reading. Thus, curve antenna will be chosen as a basic design for the transmitter. From this basic curve transmitter design, an improved transmitter with four combination of curve transmitter has been fabricated which is also known as Quadrapole Antenna. As far as first objective is concern, the effect of magnetic field strength over the distance has been improved. Prototype testing with magnetic feeders has given an improvement about 445.76% as compared to Quadrapole Antenna without the magnetic feeders. As a result, the SBL can go into deep water hydrocarbon exploration.

5.2 Recommendations

Several improvements are needed for the future works. These suggestions are issued to make sure the transmitter can perform accurately by considering all factors. For the next future planning, it is recommended to conduct the experiments in confined space to avoid noise and interference with unwanted signal. The effect of surrounding such as hand phone signal, physical movements and others related to interference need to be taken into consideration because all these effect eventually have impact on the magnetic field measurement.

Besides, in order to achieved more accurate result in the future, it is strongly recommended to used CST Software to simulate exactly as the prototype design so that, the results from both simulation and experimental can be compared to validate the results.

REFERENCES

[1] M. Espinosa Penaa, A. Manjarrez, A. Camperob. Distribution of vanadyl porphyrins inheavy crude oil a Mexican offshore. Vol.46 pp. 171-182, 1995.

[2] Tompkins, M et. al. Electromagnetic Surveying For Hydrocarbon Reservoir. U.S. Patent 7483792, 2007.

[3] Anwar Bhuiyan, Tor Wicklund and Stale Johansen. High-Resistivity Anomalies at Modgunn Arch in the Norwegian Sea. Vol. 24, January 2006.

[4] Remote sensing of hydrocarbon layers by seabed logging (SBL): Results from a cruise offshore Angola, retrieved from http://marineemlab.ucsd.edu/resources/Pubs/LeadingEdge2002.pdf, September 2010.

[5] Jonny Hesthammer, Aris Stefatos, and Mikhail Boulaenko, Rocksource Stein Fanavoll and Jens Danielsen, EMGS. CSEM performance in light of well results.

[6] Løseth, H.M. Pedersen, T. Schaug-Pettersen, S. Ellingsrud and T. Eidesmo. A scaled experiment for the verification of the SeaBed Logging method L.O. Vol. 64 (3-4) pp. 47-55, 2008.

[7] T.Eidesmo, S.Ellingsrud, M.C., S.Johansen, and Mitet Rune. Seabed Logging Heads Advances in Long-offset Electromagnetic Surveying. Oil and Gas Journal, Vol.103, June 2006.

[8] Rocksource. EM in Exploration, retrieved from http://www.rocksource.com, August 2010.

[9] T.Eidesmo,S.Ellingsrud,L.M.MacGregor,S.Constable,M.C.Sinha, S.Johansen, F.N. Kong and H.Weterdahl. Remote Detection of hydrocarbon filled layers using marine controlled source electromagnetic sounding. by EAGE 64th Conference & Exhibition – Florence, Italy, 27-30 May 2002.

[10] Anwar Bhuiyan, Tor Wicklund, and Stale Johansen. High-resistivity anomalies at Modgunn arch in the Norwegian Sea. Vol. 24, January 2006.

[11] F. N. Kong, Harald Westerdahl, Svein Ellingsrud, Terje Eidesmo and Stale Emil Johansen. Seabed logging: A possible direct hydrocarbon indicator for deepsea prospect using EM energy. Oil and Gas Journal, 13 May 2002.

[12] StatoilHydro . About Seabed Logging, retrieved from http://www.statoilhydro.com, November 2010.

[13] L.O Loseth, H.M. Pedersen, T.Schaug-Pettersen, S.Ellingsrud, and T.Eidesmo. The first test of the Seabed Logging method. Submitted to Journal of Applied Geophysics.

[14] Nur Intan Marlyny. Simulation and Design Transmitter for Seabed Logging (SBL). Degree Thesis, Universiti Teknologi PETRONAS, 2010.

[15] Halfdan Carstens. The same PRINCIPLE as in borehole logging. GEO ExPro, June 2004.

[16] Norman J. Hyne. Nontechnical Guide To Petroleum Geology, Exploration, Drilling, And Production. Pinwheel Corporation pp. 213 , 2001.

[17] Shell Exploration and Production. Deepwater Challenges. Page 9, EP Technology-Vol. 2 (1), 2007.

[18] Waves of Information, retrieved from www.emgs.com/content, November 2010.

[19] Dirt Smit and Paul R. Wood. Experience is crucial to expanding CSEM use. World Oil Journal, September 2006.

[20] Perry A. Fischer. New EM technology offering are growing quickly. World Oil Vol. 226 (6), 2005.

[21] Kurang Mehta, Misac Nabighian Yaoguo Li, Controlled Source Electromagnetic (CSEM) technique for detection and delineation of hydrocarbon reservoirs: an evaluation Center for Gravity, Electrical & Magnetic Studies, Colorado School of Mines; Doug Oldenburg, UBC-GIF, University of British Columbia.

[22] Mei Wang, Ming Deng, Qisheng Zhang and Kai Chen. The Study on Synchronization Technology for Marine Controlled Source Electromagnetic Survey, the Ninth International Conference on Electronic Measurement & Instruments, ICEMI, 2009.

[23] J. Whaley. CSEM continues to stride forward. GeoExpro, 2008.

[24] T.Eidesmo,S.Ellingsrud,L.M.MacGregor,S.Constable,M.C.Sinha, S.Johansen, F.N. Kong and H.Weterdahl. Sea Bed Logging (SBL), a new method for remote and direct identification of hydrocarbon filled layers in deepwater areas. Vol. 20 (3), 2002.

[25] Farelly.B. Remote characterization of hydrocarbon filled reservoirs at the Troll Field by Sea Bed Logging. EAGE Fall Research Workshop, Rhodes, Greece, 2004.

[26] Griffiths, D.J., Introduction to Electrodynamics (3rd ed.). Upper Saddle River, New Jersey: Prentice Hall,1999.

[27] Electromagnetic waves retrieved from http://www.amazingrust.com/Experiments/background_knowledge/ Spectroscopy.html, December 2010.

[28] Electromagnetics for Engineers , Fawwaz T.Ulaby, 2008.

[29] Masafumi Itagaki, Takaaki Fukunaga. Boundary element modelling to solve the Grad–Shafranov equation as an axisymmetric problem. Vol. 30 pp.746–757, 2006

[30] Frederick David Tombe, Belfast, Northern Ireland, United Kingdom. Lenz's Law. The General Science Journal, Ormoc City, Philippines, December 2008.

[31] Maxwell's Equations and Electromagnetic Waves, retrieved from http://galileoandeinstein.physics.virginia.edu/more_stuff/Maxwell_Eq.html, July 2010.

[32] Karl J.Ellefsen, Jared D.Abraham, David L. Wright and Aldo T.Mazzela. Numerical Study of Electromagnetic Waves Generated by a Prototype Dielectric Lagging Tool.

[33] Shahbender, Babah. Wendt, Frank.S; Gordon, Irwin Gries, Robert J. Television Receiver Ferroresonant High Voltage Power Supply Using Temperature Stable Core Material.

[34] Vishal Bhavsar, Nicholas Blas, Huy Nguyen, Alexander Balandin. Measurement of Antenna Radiation Patterns. EE117 Laboratory Manual, UC-Riverside, 2000.

[35] Antenna-Theory.com – Directivity, retrieved from www.antennatheory.com/basics/directivity.php, January 2011.

[36] Rudy Severns N6LF, Skin Depth and Wavelength in Soil, retrieved from www.antennabyn6lf.com, January 2011.

[37] Maxwell, J.C, A Dynamic Theory of the EM Field, 1864.

[38] Rudy Severns N6LF, Skin Depth and Wavelength in Soil, retrieved from www.antennabyn61f.com, January 2011.

[39] B. K. Bhattacharyya. Input Resistances of Horizontal Electric and Vertical Magnetic Dipoles Over a Homogenous Ground. IEEE Transactions on Antennas and Propagation, May 1963.

[40] V.H. Ransom , W. Wang, M. Ishii. Use of an ideal scaled model for scaling evaluation. Vol. 186, pp.135–148, 1998.

[41] CST EM STUDIO, retrieved from http://www.cst.com/Content/Products/EMS/Overview.aspx, February 2011.

[42] Ronold W. P. King. Antennas in Material Media Near Boundaries with Application to Communication and Geophysical Exploration, Part I: The Bare Metal Dipole. IEEE Transactions on Antennas and Propagation, Vol. 34 (4), April 1986.

[43] Rune Mittet and Tor Schaug-Pettersen. Shaping optimal transmitter waveforms for marine CSEM surveys. Geophysics.Vol. 37 (3), June 2008.

[44] Nur Intan Baizura. Development of Powerful Twin Antenna for Hydrocarbon Exploration. BSc. Thesis, Universiti Teknologi PETRONAS, 2009.

[45] De Hop, A.T. Handbook of radiation and scattering of waves. Academic press London, 1995.

[46] John A. Bell. Method of producing a continuously processed copper rod. Patended Oct. 31, 1967.

[47] Chave, A.,C.S.Cox. Electromagnetic Lateral Waves Observed by Earth-sounding Radars. Geophysics Journal, Vol. 41, pp. 1126-1132, 1986.

[48] R.W.P King and G.Smith. Antennas in Matter. MIT Press, 1987.

[49] Nathalie Revol and Jean-Louis Roch. Parallel Evaluation of Arithmetic Circuits. Vol. 162, pp. 133-150, 1996.

[50] Antenna Directivity and Effective Area, retrieved from http://farside.ph.utexas.edu, March 2011.

[51] Joseph J. Carr. Practical Antenna Handbook. Fourth Edition, New York, McGraw-Hill, 2001.

[52] F.N Kong and H. Westerdahl. Excitation of a Long Wire Antenna. Tenth International Conference on Ground Penetrating Radar, 21-24 June 2004.

[53] T.A.Milligan. Modern Antenna Design. Second Edition, IEEE Press, 2005.